RADIATIVE PROCESSES OF ENTANGLED DETECTORS IN ROTATING FRAMES

GABRIEL PICANÇO COSTA

Centro Brasileiro de Pesquisas Físicas (CBPF)

June 2020

"RADIATIVE PROCESSES OF ENTANGLED DETECTORS IN ROTATING FRAMES"

GABRIEL PICANÇO COSTA

Dissertação de Mestrado em Física, apresentada no Centro Brasileiro de Pesquisas Físicas do Ministério da Ciência, Tecnologia, Inovações e Comunicações. Fazendo parte da banca examinadora os seguintes professores:

Nami Fux Svaiter

Nami Fux Svaiter - Presidente/Orientador/CBPF

Reinaldo de Melo e Souza

Reinaldo Faria de Melo e Souza - UFF

Fernando da Rocha Vaz Bandeira de Melo - CBPF

Rio de Janeiro, 01 de julho de 2020.

GABRIEL PICANÇO COSTA

RADIATIVE PROCESSES OF ENTANGLED DETECTORS IN ROTATING FRAMES

Gabriel Picanço Costa: *Radiative Processes of Entangled Detectors in Rotating Frames*, June 2020

Advisor: Nami Fux Svaiter

ABSTRACT

In this thesis, we investigate the radiative processes of accelerated entangled two-level systems. First, we make a historical review of approaches for relativistic rotation. After that, we summarize important results of Quantum Field Theory in both Minkowski and general spacetimes, and we quantize a scalar field in a non-inertial, rotating frame. Using first-order perturbation theory, we then evaluate transition rates of two entangled Unruh-DeWitt detectors rotating with the same angular velocity and interacting with a massive scalar field. Decay processes for arbitrary radius, angular velocities, and energy gaps are analyzed. We discuss the mean-life of entangled states and entanglement harvesting and degradation. We found out that for similar radial coordinates, that is, $r_1 \approx r_2$, the system of detectors prepared in the common excited state shows entanglement harvesting, as it decays preferentially to the symmetric Bell state. In this regime, we also find that a system prepared in the anti-symmetric Bell state tends to be stable. In any other situation, systems prepared in an entangled state show entanglement degradation, as they decay to the non-entangled common ground state of the detectors.

Keywords: Rotating Frames, Unruh-DeWitt Detectors, Entanglement

RESUMO

Nessa tese, investigamos processos radiativos de sistemas de dois níveis acelerados e emaranhados. Primeiramente, fazemos uma revisão histórica de abordagens para rotações relativísticas. Depois disso, resumimos resultados importantes de Teoria Quântica de Campos, tanto para espaços-tempo de Minkowski quanto mais gerais, e quantizamos um campo escalar em um referencial girante, não-inercial. Usando teoria de perturbação de primeira ordem, nós então calculamos taxas de transição de dois detectores de Unruh-DeWitt emaranhados, girando com a mesma velocidade angular e interagindo com um campo escalar massivo. Processos de decaimento são analisados para diferentes raios, velocidades angulares e diferenças de energia. Também discutimos meias-vidas de estados emaranhados, assim como coleta e degradação de emaranhamento. Para coordenadas radiais similares, isto é, $r_1 \approx r_2$, verificamos que um sistema de dois detectores, ambos preparados no estado excitado, apresenta coleta de emaranhamento, pois o sistema decai preferencialmente para o estado emaranhado simétrico de Bell. Também nesse regime, verificamos que um sistema preparado no estado emaranhado anti-simétrico de Bell tende à estabilidade. Em qualquer outro caso, sistemas preparados em um estado inicial emaranhado apresentam degradação de emaranhamento ao decair para o estado fundamental comum dos detectores, não-emaranhado.

Palavras-chave: Referenciais Girantes, Detectores de Unruh-DeWitt, Emaranhamento

PUBLICATIONS

[1] Gabriel Picanço, Nami F. Svaiter, and Carlos A.D. Zarro. "Radiative Processes of Entangled Detectors in Rotating Frames." In: (2020). arXiv: 2002.06085 [hep-th].

ACKNOWLEDGMENTS

The acknowledgments are going to be written in Portuguese, to address who they concern.

À Hellen Fortes da Silva Sales, muito obrigado por ser minha companheira durante todo esse tempo, sempre me apoiando e dando suporte durante toda a minha formação, e por me ajudar a me tornar um ser humano cada vez melhor, em todos os aspectos possíveis. Sem você eu já teria me perdido no meio do caminho há muito tempo.

Ao Antonio José Soares Madeira Domingues, grande amigo e eterno mestre, pela amizade, pelos conselhos e broncas e por ter me mostrado minha vocação, e insistido que eu a seguisse da forma menos conturbada o possível. A segunda pessoa sem a qual eu certamente teria me perdido.

A meus pais, Christianne Sant'Anna Picanço e Ricardo da Silva Costa, e à minha saudosa avó, Marilda Alves de Sant'Anna, por terem tido a paciência (quase sempre) de me criar, e sempre terem apoiado minhas decisões, por mais insensatas que parecessem a princípio.

À Ana Lúcia Fortes da Silva, por ter cuidado de mim como se seu filho fosse ao longo desses anos todos, sempre com grande zelo e carinho.

Em memória de meu irmão, Leonardo Américo Sant'Anna Picanço, e de meu tio, Paulo Sávio da Silva Costa, que sempre me inspiraram com relação a diversos aspectos complementares, cada um de sua maneira única.

A Nami Fux Svaiter, por me orientar e me encaminhar nessa jornada para me tornar parte da comunidade de pesquisadores em Física Teórica.

A Carlos Augusto Domingues Zarro, por ser meu "co-orientador informal" e meu amigo ao longo desses anos, sempre me instruindo ao longo da graduação e do mestrado.

A todos os outros professores que contribuíram com minha formação, em especial Carlos Farina de Souza, Reinaldo Faria de Melo e Souza e Sebastião Alves Dias, com quem sempre pude contar quando precisava conversar sobre algo para tornar as ideias mais claras, tanto sobre questões dentro da física quanto fora dela.

A meus amigos da Matemática Aplicada e da Física da UFRJ e do CBPF, por terem trilhado esse início de carreira acadêmica comigo, algumas horas mais próximos, outras mais distantes. Pelas super-interessantes e intermináveis conversas diletantes, que tanto abriram meus horizontes e me ajudaram em momentos de dúvida. Em especial, ao Leonardo Gama Assumpção por, além do supracitado, ter me guiado com maestria por todas as ferramentas computacionais que precisei ao longo do mestrado.

A meus amigos de infância e adolescência, por todo o companheirismo ao longo desses anos todos, e, tenho certeza, dos muitos outros que estão por vir.

Ao Centro Brasileiro de Pesquisas Físicas (CBPF) e à Universidade Federal do Rio de Janeiro (UFRJ), centros de pesquisa de excelência que tanto contribuíram para minha formação.

Ao Colégio Militar do Rio de Janeiro (CMRJ) pela ótima formação que me foi dada quando jovem, e aos professores da turma IME-ITA do Sistema Elite de Ensino, por abrirem meus olhos com relação a inúmeras discussões maravilhosas nas diferentes matérias, e por me mostrar como o magistério pode ser divertido, enriquecedor e gratificante.

À Coordenação de Aperfeiçoamento de Pessoal de Nível Superior (CAPES), agência que financia o programa de pós-graduação do Centro Brasileiro de Pesquisas Físicas (CBPF); ao Conselho Nacional de Pesquisa e Desenvolvimento (CNPq), pelo financiamento durante o primeiro ano de mestrado (processo nº 134522/2018-4); e à Fundação de Amparo à Pesquisa do Rio de Janeiro (FAPERJ), pela Bolsa Nota 10 ao longo do segundo ano de mestrado (processo nº 201.810/2019, dando assim condições de que esse trabalho pudesse ser realizado com sucesso.

A André Miede e Ivo Pletikosić por seu excelente pacote *classicthesis*, usado para a formatação desta tese (disponível em https://bitbucket.org/amiede/classicthesis/).

CONTENTS

1

INTRODUCTION

Quantum information is a very important topic of research in physics nowadays, whether for studying fundamental theories, experiments, or even applications, such as in quantum computers or quantum cryptography [1]. Specifically, relativistic quantum information is becoming increasingly more relevant [2, 3, 4, 5, 6, 7, 8, 9, 10, 11, 12]. The description of detectors coupled to quantum fields claims for the relativistic approach, with measurable effects. One of them is entanglement degradation [13, 14], where correlated states turn into uncorrelated ones, for example by an interaction with a quantum field. This is very relevant since we never entirely control the coupling of a system to the environment in realistic experiments. Another effect is the entanglement harvesting [15, 16, 17], where uncorrelated objects turn into correlated ones by some other interaction, for example with a quantum field. The interpretation of this phenomenon is that correlations between different points in space-time are shown by a quantum field in the vacuum state, and a system coupled with this field can extract entanglement from that. We will show later that we can use the framework of quantum field theory to show that both effects should happen in a pair of coupled Unruh-DeWitt detectors in a rotating frame.

The possibilities of applications of field theory in our understanding of nature are enlarged by developments in the general theory of quantization of fields in curved space-times. In canonical quantization, the original construction where quantum states support an irreducible unitary representation of the Poincaré group must be modified. In this scenario, we may use arbitrary frames for quantization, even in flat space-time, as laboratories of investigations, as the vacuum states of quantum fields can be observer-dependent [18]. The quantization performed by uniformly accelerated observers in Minkowski spacetime is quite an instructive situation. The usual approach for this problem is to quantize a scalar field using Rindler's coordinate system, that is, in the Rindler frame. Both quantizations, in a Rindler frame and an inertial frame, are unitarily non-equivalents. This can be deduced by analyzing the Bogoliubov's β coefficients between Rindler and Minkowski field modes. One can also state that the definition of elementary particles and vacuum states for inertial and accelerated observers are distinct by computing the response function of a particle detector [19, 20, 21, 22]. If one prepares a uniformly accelerated detector interacting with a scalar field prepared in the Poincaré invariant (Minkowski) vacuum it will measure a thermal bath, with the temperature being proportional to its proper acceleration. This is known as the Unruh-Davies effect. Some results of quantum field theories in curved space-times, such as the Hawking effect [23], are thus anticipated by the Unruh-Davies effect.

Treatments for radiative processes of detectors in a non-inertial rotating frame [24] can be found in references [25, 26, 27, 28, 29]. Letaw and Pfausch indicated that physical content coming from the Bogoliubov's β coefficients between the rotating and the inertial modes and the response function of the detector would be in disagreement. The rotating vacuum and the Minkowski vacuum are unitarily equivalent since the Bogoliubov's β coefficients between the rotating and the inertial modes are zero. Notwithstanding, the rotating detector interacting with a scalar field in the Minkowski vacuum presents a non-zero response function for excitations. This issue was solved by Davies et al [30], as we discuss later. In addition to this incompatibility between the Bogoliubov coefficients and the response function approaches, other more fundamental problem arises. How to address rotation in a relativistic scenario?

Since the birth of Einstein's Special Relativity, the problems of rotation in a relativistic scenario have been attracted many physicists, as Ehrenfest, Born, Planck, Kaluza, Einstein, and others [31, 32, 33, 34, 35]. A very important experimental result to guide this discussion is the so-called Sagnac effect [36, 37], which is similar to the Michaelson-Morley experiment, but with light rays going through an approximated circular path instead of linear ones. Although it was discovered in 1913, it is usually evoked in the context of interferometry, while the discussion of a fundamental theory of relativistic rotation remains an unsolved issue.

In this work, we study two Unruh-DeWitt detectors [38] rotating around the origin with the same angular velocity and interacting with a massive scalar field. Radiative processes and quantum entanglement for rotating systems are discussed. Using first-order perturbation theory, the response functions of the detectors are computed, looking for the transition rate of excitations or de-excitations between any two arbitrary states. In addition, we compute the mean life of entangled states of the two detectors. Quantum entanglement and quantum harvesting are also discussed in the analysis. We also try to unravel the relevance of all the different parameters in the response function.

This thesis is organized as follows. In chapter 2 we make a brief historical review of different approaches for relativistic rotation and we discuss a specific approach to be used later. In chapter 3 we summarize important results of Quantum Field Theory in both Minkowski and general spacetimes, and we quantize a massive scalar field in the radially-bounded spacetime, in rotating cylindrical coordinates. In chapter 4 we discuss Unruh-DeWitt detectors and calculate transition rates of two entangled rotating detectors. In chapter 5, we study the transition rates, stressing the importance of all relevant parameters, and derive the expression for the mean life of entangled states, discussing its stability. In chapter 6 we present the conclusions and present possible continuations for this work.

Throughout the text, we use $\hbar = c = 1$, unless in chapter 2, where we keep c for the sake of the discussion. The signature of the Minkowski metric $\eta_{\mu\nu}$ in this work is $(+---)$.

2 RELATIVITY IN ROTATING FRAMES

In this chapter, we will briefly discuss some of the most used approaches to tackle relativistic rotation. This chapter has no intention of exhausting the subject. For this purpose, we refer the reader to reference [24].

2.1 HISTORICAL REVIEW

In Einstein's discussions about relativistic rotation [39], he assumed the surrogate rods postulate [40] to analyze a rotating disk, such that its rim would be Lorentz contracted. In this situation, the value of its circumference divided by the diameter would not be equal to π, so he concluded that the geometry of the rotating disk should be non-Euclidian. As we will see, the problem here lies within the validity of the surrogate rods postulate in a non-time orthogonal frame.

Landau and Lifshitz [41] used the transformation law between the cylindrical coordinate system adapted to an inertial frame, and another coordinate system adapted to a rotating one, which is valid only for $r < c/\omega$. In order to extend this coordinate system to any radius, that is, trying to solve the problem of tangential velocity being greater than c for radius $r > c/\omega$, Trocheries and Takeno [42, 43] define a coordinate system adapted to the rotating frame where the tangential velocity is $v/c = \tanh(\omega r/c)$, which only tends asymptotically to c. Consequences of this transformation in field theory are discussed in [44, 45, 46]. This choice is not able to reproduce experimental results, for instance, the Sagnac's effect [36, 37].

Another proposal was discussed by Grøn [47, 48]. It is able to reproduce Sagnac's effect, but it also has a discontinuity in the time coordinate, for closed circuits around the origin. Grøn also argues that the Riemann tensor associated with the spatial metric [41] in rotating coordinates is not identically zero, that is, the rotating disk should not be flat. But the construction of the spatial metric depends on exchanging light rays between two worldlines and assumes that c is invariant, which is not compatible with Sagnac's effect.

Adler, Bazin, and Schiffer [49] proposed, in their book, an infinitesimal time coordinate transformation that would transform the metric into a time orthogonal form. As stated by the authors themselves, the differential of the new time coordinate is not exact, that is, one would not be able to correctly define the time coordinate. An alternative extension of special relativity for rotating frames was developed by Klauber [50].

2.2 KLAUBER'S THEORY

It is common to assume that c is invariant under any kind of transformation, based on experimental evidence such as Michaelson-Morley experiments, and the success of Einstein's special relativity. Although, as Sagnac showed in 1913, this invariance does not remain in rotating frames. In a disk with radius r and angular velocity ω, Sagnac measured the speed of light in a rotating frame to be equal to $c_{rot} = c(1 \pm \omega r/c)$, up to first order in $\omega r/c$. The signal depends if the light ray is emitted in the same direction as the velocity of the rim, or in the opposite direction.

If one assumes the previous formula for the speed of light in a rotating frame as a postulate instead of assuming its invariance, one is able to construct a theory of relativity for rotations that will be consistent with the usual approach of quantum field theory to rotating systems, as we will see. Let us write Klauber's postulates [50]:

- **Postulate 1)** For a disk of radius r rotating with angular velocity ω, and as many mirrors as necessary in its rim, the speed of light in the rotating frame tends to $c_{rot} = c \pm \omega r$ as the trajectory of the light ray tends to a circunference.

- **Postulate 2)** There is a privileged frame, the non-rotating one. Every rotating frame can perform local experiments to detect that it is in fact rotating, and they all can distinguish the non-rotating frame univocally.

- **Postulate 3)** The line element ds^2 is invariant, regardless of any transformation of coordinates performed.

The second postulate is similar in some sense to Newton's bucket argument, which establishes that rotation is absolute, unlike translation. The third postulate is necessary if the spacetime should be able to be described by differential geometric methods. From the above postulates, we can draw the following conclusions:

- **Simultaneity:** we can analyze Einstein's *Gedankenexperiment* on the simultaneity of events under the light of the above postulates. Instead of thinking in an observer in the ground and other inside a moving train, let us imagine an observer fixed on the center of the disk and other one fixed on its rim. As we now have a Galilean-like composition of velocity for light, one reaches the trivial conclusion that the simultaneity is the same for both observers.

- **(Lack of) Lorentz contraction:** by the third postulate, ds^2 is the same for an inertial frame, with cylindrical coordinates (T, R, Φ, Z), and for a rotating frame, with cylindrical coordinates (t, r, φ, z). So, we get $ds^2 = c^2 dT^2 - dL^2 = c^2 dt^2 - dl^2$, where dL and dl are the spatial differential coordinates in the inertial and rotating frames, respectively. As both frames share simultaneity, $dT = 0 \to dt = 0$, and we get $dL = dl$. Therefore, there is no Lorentz contraction as we change from the non-rotating to the rotating frame.

- **Proper time:** since there is no spatial contraction, a rotating and a non-rotating observers will both see the rim of the disk with equal length $2\pi r$, and both of them can detect that the disk rotates with angular velocity ω. Let us calculate the proper time of an observer on the rim:

$$c^2\Delta\tau^2 = \Delta s^2 = c^2\Delta T^2 - (\omega r\Delta T)^2 \to \quad (2.1)$$

$$c^2\Delta\tau^2 = c^2(1-\frac{\omega^2 r^2}{c^2})\Delta T^2 \to \Delta\tau = \sqrt{(1-\frac{\omega^2 r^2}{c^2})}\Delta T. \quad (2.2)$$

Inspired by Einstein's relativity, let us define $\gamma = 1/\sqrt{1-\omega^2r^2/c^2}$. One can see that, despite the proper time showing a $1/\gamma$ factor, Lorentz time transformation is not symmetric as it is in special relativity. The time for an observer with greater radial coordinate runs necessarily slower, as in the twins' paradox. It relates to the fact that observers in the rotating frame experience acceleration. An observer on the rim of the disk experiences a centripetal acceleration, as well as, in the twins' paradox, the person in the spaceship experiences accelerations.

Assuming the third postulate, the invariance of ds^2 under general coordinate transformations, one can show that the other two postulates are equivalent to a certain rule for changing coordinates between inertial and rotating cylindrical coordinates, as follows:

$$\begin{aligned} T &= t, && (2.3)\\ R &= r, && (2.4)\\ \Phi &= \varphi + \omega t, && (2.5)\\ Z &= z, && (2.6) \end{aligned}$$

The line element in inertial cylindrical coordinates reads

$$ds^2 = c^2dT^2 - dR^2 - R^2d\Phi^2 - dZ^2. \quad (2.7)$$

We can now substitute the inertial coordinates for the rotating ones, and then we get the metric

$$ds^2 = c^2\left(1-\omega^2r^2/c^2\right)dt^2 - dr^2 - r^2d\varphi^2 - dz^2 - 2\omega r^2 d\varphi dt. \quad (2.8)$$

These coordinate transformations are exactly the ones assumed in papers that work with quantum field theories in rotating coordinates, as [25, 26, 30]. It's worth noticing that, until now, Klauber's theory remains consistent with electrodynamics' results [51], and with other experiments related to relativistic rotation, such as Phipps' [52], Brillet and Hall's [53, 54] and cyclotron experiments [50]. One obvious downside of Klauber's theory is that it contains supra-luminal velocities for $r > c/\omega$, where the sign of the g_{00} element of the metric changes. We will discuss this issue in section 3.3.

For completeness, let us derive the speed of light in the rotating frames, from the metric (2.8). As we are only interested in the speed of light across the rim of the disk, we will impose $dr^2 = dz^2 = 0$. Now, in a lightlike path, $ds^2 = 0$. Substituting these conditions into (2.8), we get

$$0 = \left(c^2 - \omega^2 r^2\right) dt^2 - r^2 d\varphi^2 - 2\omega r^2 d\varphi dt \;\rightarrow\; \frac{r d\varphi}{dt} = c \pm \omega r. \quad (2.9)$$

One can call this expression the *coordinate* speed of light. Using equation (2.1), one can use the proper time to define the *physical* speed of light on the rim of the disk to be

$$\frac{r d\varphi}{d\tau} = \frac{c \pm \omega r}{\sqrt{1 - \frac{\omega^2 r^2}{c^2}}} = c \pm \omega r + \mathcal{O}\left(\frac{\omega r}{c}\right)^2. \quad (2.10)$$

It is interesting to notice that it is the g_{0i} term in the metric which is responsible for the non-invariance of the speed of light. If we had a stationary spacetime, even with $g_{00} \neq 1$, the physical speed of light would be invariant and equal to c.

3 QUANTUM FIELD THEORY IN CURVED SPACES

Quantum Field Theory is the suitable formalism to calculate the radiative processes of particle detectors. In particular, as we will study a system in a non-inertial frame, we have to take into account the effects of the non-Minkowskian metric tensor in the formalism, that is, we are going to use the formalism developed to study Quantum Field Theory in Curved Spaces (QFTCS). Before going into the problem of detectors in circular uniform motions, let us make a short passage from QFT to QFTCS. This chapter follows reference [21]. See also [55, 56, 57, 58, 59].

3.1 QFT WITH MINKOWSKI METRIC

In this section, we will discuss QFT in cartesian coordinates of an inertial frame, with Minkowski metric. Let $\varphi(t, \mathbf{x}) = \varphi(x)$ be a free real scalar field in $\mathbb{R}^{n+1}$, where t is the time coordinate, $\mathbf{x}$ is the spatial n-dimensional vector and x^μ is the spacetime $(n+1)$-dimensional vector. In other words, $\mathbb{R}^{n+1}$ is a flat Lorentzian manifold. The usual free Lagrangian density $\mathcal{L}$ and the action $\mathcal{S}$ read

$$\mathcal{L}(\varphi)(x) = \frac{1}{2}\partial_\mu\varphi\partial^\mu\varphi - m^2\varphi^2; \qquad \mathcal{S}[\varphi] = \int d^{n+1}x\ \mathcal{L}(\varphi)(x), \tag{3.1}$$

where $\partial_\mu\varphi = \partial\varphi/\partial x^\mu$, $\partial^\mu\varphi = \eta^{\mu\nu}\partial_\nu\varphi$, and m is the mass of the field. In the above expression $\mathcal{L}(\varphi)(x)$ depends on the Taylor expansion of φ at x. Let us impose that the action is extremized to obtain the equation of motion for the field:

$$\frac{\delta\mathcal{S}}{\delta\varphi(x)} = 0 \quad \rightarrow \quad \left(\Box + m^2\right)\varphi(x) = 0, \tag{3.2}$$

where $\Box = \partial_\mu\partial^\mu$. The last equation is called the Klein-Gordon equation. A set of solutions (also called *modes*) $u_\mathbf{k}$ indexed by n-dimensional vectors $\mathbf{k}$ can be given by

$$u_\mathbf{k} = e^{-i\omega t + i\mathbf{k}\cdot\mathbf{x}}, \tag{3.3}$$

where $\omega_\mathbf{k}^2 = \mathbf{k}^2 + m^2$. If we define the $(n+1)$-dimensional vector $k^\mu = (\omega_\mathbf{k}, \mathbf{k})$, the solutions can be written as

$$u_\mathbf{k} = e^{-ikx}. \tag{3.4}$$

We can define a scalar product between fields in a similar way as we define it between wave functions in quantum mechanics, that is:

$$\langle\varphi, \phi\rangle = i\int d^n\mathbf{x}\ [(\partial_t\varphi(x))\phi^*(x) - \varphi(x)(\partial_t\phi^*(x))]. \tag{3.5}$$

Note that we are integrating in an hyperplane of simultaneity at some fixed time t. With this scalar product, the $u_{\mathbf{k}}$ modes are orthogonal:

$$\langle u_{\mathbf{k}}, u_{\mathbf{k}'} \rangle = 0, \quad \text{for } \mathbf{k} \neq \mathbf{k}'. \tag{3.6}$$

Rescaling the modes as

$$u_{\mathbf{k}} = \frac{e^{-ikx}}{\sqrt{2\omega_{\mathbf{k}}(2\pi)^n}} \tag{3.7}$$

we finally obtain

$$\langle u_{\mathbf{k}}, u_{\mathbf{k}'} \rangle = \delta^{(n)}(\mathbf{k} - \mathbf{k}'), \quad \langle u^*_{\mathbf{k}}, u^*_{\mathbf{k}'} \rangle = -\delta^{(n)}(\mathbf{k} - \mathbf{k}') \\ \text{and} \quad \langle u_{\mathbf{k}}, u^*_{\mathbf{k}'} \rangle = \langle u^*_{\mathbf{k}}, u_{\mathbf{k}'} \rangle = 0. \tag{3.8}$$

Now, we define positive (negative) frequency modes with respect to the time t solutions of the equation of motion that are eigenfunctions of the operator $\partial/\partial t$, with a purely imaginary eigenvalue, with negative (positive) imaginary part. That is, if

$$\frac{\partial u(x)}{\partial t} = -i\,\omega\, u(x), \tag{3.9}$$

$u(x)$ is called a positive frequency mode if $\omega > 0$, and a negative frequency mode if $\omega < 0$. It is immediate to see that the modes $u_{\mathbf{k}}$ are positive frequency modes with respect to t, and $u^*_{\mathbf{k}}$ are negative frequency modes with respect to t.

It is useful to expand the field $\phi(x)$ in a basis of normal modes, as follows:

$$\phi(x) = \sum_{\mathbf{k}} \left[a_{\mathbf{k}} u_{\mathbf{k}}(x) + a^*_{\mathbf{k}} u^*_{\mathbf{k}}(x) \right]. \tag{3.10}$$

Defining $\Pi(x)$ as the canonical conjugated field given by $\Pi := \partial\mathcal{L}/\partial(\partial_t\phi)$, we can now proceed with the second quantization by promoting ϕ and Π to operators and imposing the following equal-time commutation relations

$$\begin{aligned} [\phi(t,\mathbf{x}), \phi(t,\mathbf{x}')] &= 0, \\ [\Pi(t,\mathbf{x}), \Pi(t,\mathbf{x}')] &= 0, \\ [\phi(t,\mathbf{x}), \Pi(t,\mathbf{x}')] &= i\delta^{(n)}(\mathbf{x} - \mathbf{x}'). \end{aligned} \tag{3.11}$$

Promoting the fields to operators is equivalent to promoting $a_{\mathbf{k}}$ and $a^\dagger_{\mathbf{k}}$ to operators in (3.10). We can also use this expansion to show that the above commutation relations are respectively equivalent to

$$\begin{aligned} [a_{\mathbf{k}}, a_{\mathbf{k}'}] &= 0, \\ [a^\dagger_{\mathbf{k}}, a^\dagger_{\mathbf{k}'}] &= 0, \\ [a_{\mathbf{k}}, a^\dagger_{\mathbf{k}'}] &= \delta^{(n)}(\mathbf{k} - \mathbf{k}'). \end{aligned} \tag{3.12}$$

The operators $a^{\dagger}_{\mathbf{k}}$ and $a_{\mathbf{k}}$ are called *creation* and *annihilation operators*, respectively. We define the vacuum state associated with the decomposition (3.10), denoted as $|0\rangle$, such that

$$a_{\mathbf{k}}|0\rangle = 0, \quad \forall \mathbf{k}. \tag{3.13}$$

We can use the creation operators to generate the so-called one-particle states:

$$|1_{\mathbf{k}}\rangle = a^{\dagger}_{\mathbf{k}}|0\rangle. \tag{3.14}$$

We can continue applying the creation operator to generate states with more particles with the same momentum k, as

$$|n_{\mathbf{k}}\rangle = \frac{(a^{\dagger}_{\mathbf{k}})^n}{(n!)^{1/2}}|0\rangle. \tag{3.15}$$

By using the third commutator of (3.12) and imposing that particle states are normalized to unity, we get

$$a^{\dagger}_{\mathbf{k}}|n_{\mathbf{k}}\rangle = (n+1)^{1/2}|(n+1)_{\mathbf{k}}\rangle \tag{3.16}$$

$$a_{\mathbf{k}}|n_{\mathbf{k}}\rangle = n^{1/2}|(n-1)_{\mathbf{k}}\rangle \tag{3.17}$$

Similarly, we generate many-particle states, with f different momenta, as

$$|n_{1,\mathbf{k}_1}, n_{2,\mathbf{k}_2}, ..., n_{f,\mathbf{k}_f}\rangle = (n_1!n_2!...n_f!)^{-1/2}\left[(a^{\dagger}_{k_1})^{n_1}(a^{\dagger}_{k_2})^{n_2}...(a^{\dagger}_{k_f})^{n_f}\right]|0\rangle. \tag{3.18}$$

If one defines $N_{\mathbf{k}} := a^{\dagger}_{\mathbf{k}}a_{\mathbf{k}}$, it is easy to see from (3.16) and (3.17) that

$$\langle n_{1,\mathbf{k}_1}, n_{2,\mathbf{k}_2}, ..., n_{f,\mathbf{k}_f}|N_{\mathbf{k}_i}|n_{1,\mathbf{k}_1}, n_{2,\mathbf{k}_2}, ..., n_{f,\mathbf{k}_f}\rangle = n_i, \tag{3.19}$$

so it is called the "number operator for mode $\mathbf{k}$". One can define the "total number operator" as

$$N = \sum_{\mathbf{k}} N_{\mathbf{k}}. \tag{3.20}$$

All the steps in this section were taken in a coordinate system adapted to an inertial frame, in Minkowski spacetime. The internal product (3.5) was defined using a derivative with respect to the time t of this coordinate system. That means that the normal modes, creation and annihilation operator, vacuum state, particle states, and number operators are all related to the Minkowski metric tensor, or, more specifically, to this coordinate system. So, we will add a M (from Minkowski) label to them, as other frames and metrics tensors would define different modes, states, and operators, as we will see explicitly in the next section. It is usual to say for instance that N_M is the total number operator *associated with the Minkowski vacuum* $|0\rangle_M$. Now, let us discuss fields and second quantization in the coordinate systems of more general frames.

3.2 QFT WITH GENERAL METRICS

In this section, we will develop the second quantization in a space with a general metric tensor. That can be the metric of a curved spacetime (from General Relativity, for example), or just a flat spacetime equivalent to Minkowski, but with a coordinate system adapted to a non-inertial frame. The formalism that we shall develop applies to both situations. We assume that the reader is acquainted with General Relativity, and refer to reference [60] and [61] for more details.

Take the spacetime to be a smooth (C^∞) globally hyperbolic pseudo-Riemannian $(n+1)$-dimensional manifold M. The line element in this manifold reads

$$ds^2 = g_{\mu\nu}(x)dx^\mu dx^\nu, \quad (\mu, \nu \in 0, 1, ..., n) \tag{3.21}$$

where the metric $g_{\mu\nu}$ has 1 positive and n negative eigenvalues.

Let us define, as usual, $g = \det g_{\mu\nu}$, and $\nabla_\mu \phi$ to be the μ-th component of the covariant derivative of ϕ. Since we are only going to use scalar fields, their covariant derivative equals their partial derivative, that is, $\nabla_\mu \phi = \partial_\mu \phi$.

Using the Principle of General Covariance, we can generalize the Minkowskian free Lagrangian, such that the most complete scalar Lagrangian density without interaction terms in ϕ reads

$$\mathcal{L}(\varphi)(x) = \frac{1}{2} g^{\mu\nu}(x)\partial_\mu \varphi(x)\partial_\nu \varphi(x) - \frac{1}{2}[m^2 + \xi R(x)]\varphi^2(x), \tag{3.22}$$

where $R(x)$ is Ricci's scalar and ξ is its coupling with the field. In this work, we will assume the *minimally coupled* situation, that is, $\xi = 0$.

We need the action to also be an invariant by coordinate transformations, so we cannot just integrate the Lagrangian density, since the volume element is not a scalar. But the product $\sqrt{-g}\, d^4x$ is, so we define the action to be

$$S[\varphi] = \int d^4x \sqrt{-g}\, \mathcal{L}(\varphi)(x). \tag{3.23}$$

By extremizing the action with respect to the field ϕ, we get its equation of motion in the minimally coupled case:

$$[\Box + m^2]\phi(x) = 0, \tag{3.24}$$

where $\Box$ is now given by $g^{\mu\nu}\nabla_\mu \nabla_\nu$ and ∇ is the covariant derivative operator. We can write $\Box\phi$ as

$$\Box\phi = (-g)^{-1/2}\partial_\mu[(-g)^{1/2} g^{\mu\nu}\partial_\nu \phi], \tag{3.25}$$

that is the expression that we are going to use later to solve the equation of motion.

In a spacetime with a general metric, to define the internal product we need to choose a Cauchy hypersurface Σ, with an orthogonal vector field n^μ. Thus, we can define

$$\langle \psi, \phi \rangle = i \int \sqrt{|h|} d\Sigma \, n_\mu [\psi^* \partial^\mu \phi - \phi \, \partial^\mu \psi^*], \tag{3.26}$$

where $d\Sigma$ is the volume element of Σ and h is the determinant of the metric induced in the hypersurface. We can now solve the equation of motion to find a complete set of modes satisfying

$$\langle u_i, u_j \rangle = \delta_{ij}, \quad \langle u_i^*, u_j^* \rangle = -\delta_{ij} \quad \text{and} \quad \langle u_i, u_j^* \rangle = \langle u_i^*, u_j \rangle = 0, \tag{3.27}$$

where i and j are sets of relevant indices specifying the modes. The modes u_i and u_i^* are called positive and negative norm modes, respectivelly, with respect to this the internal product (3.26).

We are now able to expand the field in the basis of normal modes, as

$$\phi(x) = \sum_i \left[a_i u_i(x) + a_i^* u_i^*(x) \right]. \tag{3.28}$$

We can again perform the second quantization by promoting ϕ, and equally a_i and a_i^*, to operators, and imposing commutation relations similar to (3.12):

$$\begin{aligned} [a_i, a_j] &= 0, \\ [a_i^\dagger, a_j^\dagger] &= 0, \\ [a_i, a_j^\dagger] &= \delta_{ij}. \end{aligned} \tag{3.29}$$

As we will only be restricted to this situation, let us assume that the metric is static. We can then define the vacuum state $|0\rangle_u$ associated with the u modes as in the Minkowski metric case, such that

$$a_i |0\rangle_u = 0, \quad \forall i, \tag{3.30}$$

and construct the Fock space by acting creation operators in the vacuum state, creating what we will call a-particle states.

If we have solved the equation of motion in other set of coordinates, for instance, we would have find a second set of normal modes v_i with which we could expand the field. Therefore, we would have other coefficients b_i, as follows

$$\phi(x) = \sum_i \left[b_i v_i(x) + b_i^* v_i^*(x) \right]. \tag{3.31}$$

We could now have defined the vacuum state $|0\rangle_v$ associated with the new modes, such that

$$b_i |0\rangle_v = 0, \quad \forall i, \tag{3.32}$$

and other basis for the Fock space, using $b_i^\dagger$ to create b-particle states.

One question that naturally arises is the relation between a- and b-particle states. Are both vacua equivalent in some sense? Does the total number operator associated with the a operators measures the number of b-particles correctly?

In a Minkowskian space, we have privileged sets of coordinates: the ones adapted to inertial frames. They are taken into each other by Poincaré group transformations, which leaves the metric tensor invariant. The vacuum and the Fock space basis elements are also invariant [21]. Remember that in quantum field theory we are dealing with countable infinite degrees of freedom. In this situation, there are many inequivalent representations of the operator algebra. Therefore the definition of vacuum state and the set of its annihilation operators are not unique. We can say that there is an infinite number of choices for the vacuum [62]. In the following, we will discuss an example that illustrates this general statement of different Fock spaces.

Following the spirit of general relativity, we should be able to equally describe physical properties in any coordinate system, including coordinates of non-inertial frames. And, under general coordinate transformations, the Fock space is in general not invariant. If one chooses another coordinate system to solve (3.24) and get another basis of normal modes, in general, this leads to a different vacuum and a different Fock space. Therefore, the particle concept in quantum field theory in curved spaces is intrinsically frame-dependent. Let us now establish relations between different Fock spaces.

One can expand the v-modes into the base of u-modes since it is complete:

$$v_j = \sum_i \alpha_{ji} u_i + \beta_{ji} u_i^*. \tag{3.33}$$

Inverting the above equation, we find

$$u_i = \sum_j \alpha_{ji}^* v_j - \beta_{ji} v_j^*. \tag{3.34}$$

Equations (3.33) and (3.34) and called Bogoliubov transformations, and α_{ji} and β_{ji} are called Bogoliubov coefficients. We can then take the internal product between the modes to explicitly find the coefficients in terms of the modes:

$$\alpha_{ji} = \langle u_i, v_j \rangle, \quad \text{and} \quad \beta_{ji} = -\langle u_i^*, v_j \rangle. \tag{3.35}$$

We can now use equations (3.28), (3.31), (3.33) and (3.34) to find relations between the creation and annihilation operators, as follows

$$a_i = \sum_j \alpha_{ji} b_j + \beta_{ji}^* b_j^\dagger \tag{3.36}$$

and

$$b_j = \sum \alpha_{ji}^* a_i - \beta_{ji}^* a_i^\dagger \tag{3.37}$$

It is easy to show that the Bogoliubov coefficients always satisfy the following relations:

$$\sum_k \alpha_{ik}\alpha^*_{jk} - \beta_{ik}\beta^*_{jk} = \delta_{ij} \tag{3.38}$$

and

$$\sum_k \alpha_{ik}\beta_{jk} - \beta_{ik}\alpha_{jk} = 0. \tag{3.39}$$

From (3.36) and (3.37), it is immediate that the vacua states are equivalent, that is,

$$a_i|0\rangle_v = 0 \quad \text{and} \quad b_i|0\rangle_u, \quad \forall i, \tag{3.40}$$

if and only if $\beta_{ij} = 0$, for all i and j.

To answer the question posed in the beginning of the discussion of Bogoliubov transformations, we can now use (3.36) to compute the expectation value of the number operator of a-particles in some mode u_i in the vacuum of v particles:

$$_v\langle 0|a_i^\dagger a_i|0\rangle_v = \sum_j |\beta_{ji}|^2, \tag{3.41}$$

that is, the vacuum of b-particles contains $\sum_j |\beta_{ji}|^2$ particles in the u_i mode, and a total of $\sum_{i,j} |\beta_{ji}|^2$ a-particles.

3.3 CANONICAL QUANTIZATION IN ROTATING COORDINATES

The discussion in this section is similar to the section 2 of reference [63]. In this section, we use cylindrical coordinates (t, r, φ, z) adapted to a rotating frame and the procedures discussed in the last section to quantize a massive scalar field in this non-inertial frame. First, as discussed in chapter 2:

$$T = t, \tag{3.42}$$

$$R = r, \tag{3.43}$$

$$\Phi = \varphi + \omega t, \tag{3.44}$$

$$Z = z, \tag{3.45}$$

where (T, R, Φ, Z) are the cylindrical coordinates of an inertial frame. The line element in the rotating frame then reads (from now on, c=1)

$$ds^2 = \left(1 - \omega^2 r^2\right) dt^2 - dr^2 - r^2 d\varphi^2 - dz^2 - 2\omega r^2 d\varphi dt. \tag{3.46}$$

From the metric (3.46), we get, as trivial Killing vectors, $\partial_t = (1, 0, 0, 0)$, $\partial_\varphi = (0, 0, 1, 0)$ e $\partial_z = (0, 0, 0, 1)$, the generators of translations on their respective directions. Since the vector ∂_t is not time-like in all spacetime, we cannot define positive and negative modes for all radial coordinate. This definition will be discussed later. This problem was solved imposing Dirichlet's boundary conditions for $r = \omega^{-1}$ [30]. Another Killing vector, time-like in all spacetime, $\partial_T = (1, 0, -\omega, 0)$, which is the generator of translation in the time coordinate adapted to inertial frames, will be useful in our discussions. In this scenario, it is natural to define an inner product for each of the possible time-like Killing vectors, K^μ, according to (3.26).

To find normal modes to expand the field, before proceeding with the quantization, we need to solve the equation of motion for the field. Substituting (3.25) and the metric (3.46) into (3.24) we get

$$\left(\partial_t^2 - \frac{1}{r}\partial_r(r\partial_r) - \left(\frac{1}{r^2} - \omega^2\right)\partial_\varphi^2 - \partial_z^2 - 2\omega\partial_t\partial_\varphi + \mu^2\right)\phi = 0, \quad (3.47)$$

where μ is the mass of the scalar field. To proceed, let us make an ansatz for the complete set of modes $u_{\varepsilon mk}$

$$u_{\varepsilon mk}(t, r, \varphi, z) \propto \exp\left(-i\varepsilon t + im\varphi + ikz\right)R(r), \quad (3.48)$$

where ε, m, and k are arbitrary constants that label the field modes (with m being integer). Substituting equation (3.48) into equation (3.47), we obtain the radial equation

$$\frac{1}{r}\frac{d}{dr}\left(r\frac{dR(r)}{dr}\right) + \left((\varepsilon + m\omega)^2 - k^2 - \mu^2 - \frac{m^2}{r^2}\right)R(r) = 0. \quad (3.49)$$

The physical acceptable solutions for the above equation are Bessel functions of first kind, J_m. Defining $(\varepsilon + m\omega)^2 - k^2 - \mu^2 = \chi^2$, the radial solution can be written as

$$J_m(\chi r) = \sum_{n=0}^{\infty} \frac{(-1)^n}{n!\Gamma(n + m + 1)}\left(\frac{\chi r}{2}\right)^{m+2n}, \quad n \in \mathbb{Z}. \quad (3.50)$$

Imposing the Dirichlet's boundary condition on some radial coordinate a, we have

$$J_m(\chi a) = 0. \quad (3.51)$$

Therefore, $\chi = \alpha_{mn}/a = k_{mn}$, where α_{mn} is the n-th root of the m-th Bessel function of the first kind. In this case, the normalization of the radial mode is given by:

$$\int_0^a dr\, r J_m(k_{mn}r) J_m(k_{ml}r) = \frac{a^2}{2}[J_m'(k_{mn}a)]^2\delta_{nl}, \quad (3.52)$$

where $J_m'(k_{mn}a) = \left.\frac{dJ_m(k_{mn}r)}{dr}\right|_{r=a}$. The normalized cylindrical modes in the rotating frame are written as

$$u_{kmn}(t, r, \varphi, z) = \frac{\exp[-i\varepsilon t + im\varphi + ikz] J_m(k_{mn}r)}{2\pi a[J_m'(k_{mn}a)]N_{kmn}}, \quad (3.53)$$

where N_{kmn} refers to the different possible normalizations given by the two time-like Killing vectors. It reads

$$N_{kmn} = \sqrt{\varepsilon}, \text{ if } K^\mu = \partial_T^\mu, \quad \text{and} \quad N_{kmn} = \sqrt{\varepsilon + m\omega}, \text{ if } K^\mu = \partial_t^\mu. \tag{3.54}$$

Since the inner products between arbitrary field modes are

$$\langle u_{kmn}, u^*_{k'm'n'} \rangle = \langle u^*_{kmn}, u_{k'm'n'} \rangle = 0 \tag{3.55}$$

and

$$\langle u_{kmn}, u_{k'm'n'} \rangle = -\langle u^*_{kmn}, u^*_{k'm'n'} \rangle = \delta(k-k')\delta_{mm'}\delta_{nn'}, \tag{3.56}$$

we say that u and u^* are positive and negative norm modes, respectively. Notice that they are also respectively positive and negative frequency modes with respect to the time coordinate adapted to the rotating frame. Introducing E such that $E^2 := (\varepsilon + m\omega)^2 = k_{mn}^2 + k^2 + \mu^2$, we get

$$\begin{aligned} -i\varepsilon t + im\varphi = -i(E - m\omega)t + im\varphi = -iEt + im(\varphi + \omega t) \\ \to -i\varepsilon t + im\varphi = -iET + im\Phi. \end{aligned} \tag{3.57}$$

In order to compare both quantizations using the inertial modes and the rotating modes, one can compute the Bogoliubov coefficients between these modes, as discussed in section 3.2. One shows that the Bogoliubov's β coefficients are zero, since

$$u_{kmn}(t, r, \varphi, z) \propto \exp[-i\varepsilon t + im\varphi + ikz] J_m(k_{mn} r) \tag{3.58}$$

and

$$U_{kmn}(T, R, \Phi, Z) \propto \exp[-iET + im\Phi + ikZ] J_m(k_{mn} R), \tag{3.59}$$

where U_{kmn} are positive frequency modes with respect to the time T of the inertial frame, in cylindrical coordinates. Therefore, the vacuum expectation value of one frame's number operator calculated in the other frame's vacuum state is always zero.

In the following, it is important to define the positive Wightman function, given by

$$G^+(x, x') = \langle 0 | \phi(x) \phi(x') | 0 \rangle. \tag{3.60}$$

For two detectors, there are going to be four positive Wightman functions, since each coordinate can be evaluated in one of the two worldlines. In a rotating frame, we can use the expansion (3.28) with modes given by (3.53) to compute

$$G^+_{jk}(x_j, x_k) = \sum_{\substack{m=-\infty,\\ n=1}}^{\infty} \int_{-\infty}^{\infty} dk \frac{J_m(k_{mn} r_j) J_m(k_{mn} r_k) e^{-i[\varepsilon \Delta t - m\Delta\varphi - k\Delta z]}}{4\pi^2 a^2 [J'_m(k_{mn} a)]^2 N_{kmn}^2}, \tag{3.61}$$

where $\Delta x^\mu = x_j^\mu - x_k^\mu$.

4

RADIATIVE PROCESSES OF UNRUH-DEWITT DETECTORS

The aim of this chapter is to discuss the Unruh-DeWitt model for particle detectors [64] and its radiative properties in rotating frames. For a didactic digression about this model for particle detectors, we refer the reader to reference [65]. Unruh-DeWitt detectors are point-like two-level systems that are coupled to a scalar field through a monopole interaction. It is a very simple model of a detector, but it is enough for many applications, as computing the Unruh effect [20]. Particle detectors are also often called "atoms", despite not having an internal structure or interacting with an electromagnetic field. In general, adding more levels to Unruh-DeWitt detectors is not going to reveal any new important features of different situations. One interesting generalization being discussed nowadays is the use of extense detectors. For this discussion, we refer the reader to [66, 67].

4.1 ONE DETECTOR

Let us begin the discussion with one detector interacting with a scalar field. The total Hamiltonian of the system is given by

$$H = H_d + H_f + H_{int}, \tag{4.1}$$

where H_d and H_f are the free detectors and field Hamiltonians, respectively. The H_{int} is the interaction Hamiltonian between the two-level system and the scalar field. The free Hamiltonian of the detector in its proper time is given by

$$H_d = \frac{E}{2}\big(|e\rangle\langle e| - |g\rangle\langle g|\big) =: \frac{E}{2}S^z, \tag{4.2}$$

where $|g\rangle$ is the ground state of the detector, and $|e\rangle$ is its excited state. These states are the eigenstates of the free Hamiltonian, with eigenvalues $-E/2$ and $E/2$, respectively. Now, the free Hamiltonian of the massive scalar field ϕ is given by

$$H_f = \frac{1}{2}\int d^3x \left[\big(\dot{\phi}(x)\big)^2 + \big(\nabla\phi(x)\big)^2 + \mu^2\phi^2(x)\right], \tag{4.3}$$

where μ is the mass of the field, the dot represents derivative with respect to t and ∇ is the gradient operator. Finally, the interaction Hamiltonian is written as

$$H_{int}(t) = \lambda\chi\big(\tau(t)\big)m\big(\tau(t)\big)\phi\big(x^{\mu}\left(\tau(t)\right)\big)\frac{d\tau(t)}{dt}, \tag{4.4}$$

where λ is the dimensionless coupling constant of the interaction, χ is a real-valued switch-function for the interaction of the detectors with the scalar field, and $m(\tau(t))$ is the monopole operator, with τ being the proper time of the detector. The field $\phi(x^\mu(\tau))$ is evaluated in the classical trajectory of each of the detectors, and the factor $d\tau/dt$ is the Jacobian to correct the time integration to its proper time value.

Using $S^+ = |e\rangle\langle g|$ and $S^- = |g\rangle\langle e|$, we can describe the monopole operator as

$$m(\tau) = m_{12}(\tau)\, S^+ + m_{21}(\tau)\, S^-. \tag{4.5}$$

For simplicity, we will take $m_{12} = m_{21} =: m$. In the interaction picture, for arbitrary initial and final states $|i\rangle$ and $|f\rangle$ of the detectors, respectively, we have

$$\langle f|m(\tau)|i\rangle = e^{i(E_f - E_i)\tau}\langle f|m(0)|i\rangle = e^{i(E_f-E_i)\tau} m_{fi}, \tag{4.6}$$

where we defined $m_{fi} := \langle f|m(0)|i\rangle$, and E_i and E_f are respectively the energies of the initial and final states of the detector.

To calculate the probability of transition between states, we use the Schrödinger equation of the interaction picture,

$$i\frac{dU(t,t_i)}{dt} = H_{int}(t)U(t,t_i), \tag{4.7}$$

such that

$$\begin{aligned} U(t,t_i) &= \mathcal{T}\left\{\exp\left(-i\int_{t_i}^{t} H_{int}(t')dt'\right)\right\} \rightarrow \\ U(t,t_i) &= 1 - i\lambda\int_{t_i}^{t_f} dt H_{int}(t) + \mathcal{O}(\lambda^2), \end{aligned} \tag{4.8}$$

where t_i is an arbitrary initial time, and $\mathcal{T}$ is the usual time-ordering operator. With the evolution operator, one can compute the transition amplitude between arbitrary states $|i\rangle$ and $|f\rangle$. We get

$$A(t_i,t_f,\phi_i,\phi_f) = (\langle f|\otimes\langle\phi_f|)U(t_f,t_i)(|i\rangle\otimes|\phi_i\rangle), \tag{4.9}$$

where $|\phi_i\rangle$ and $|\phi_f\rangle$ are the initial and final states of the scalar field. Assuming the initial state of the field as the vacuum state, $|\phi_i\rangle = |0\rangle$, and tracing out $|\phi_f\rangle$, we get that the probability of transition can be written as

$$\begin{aligned} P_{|0\rangle;i\to f}(t_f,t_i) = \lambda^2 \int_{t_i}^{t_f} dt \int_{t_i}^{t_f} dt' |m_{fi}|^2 \langle 0|\phi\big(x^\mu(\tau)\big)\phi\big(x'^\mu(\tau')\big)|0\rangle \\ \times \frac{d\tau(t)}{dt}\frac{d\tau(t')}{dt'} e^{-i(E_f-E_i)(\tau-\tau)}\chi(\tau)\chi(\tau'). \end{aligned} \tag{4.10}$$

This probability of transition is the product of the coupling constant with two factors: the selectivity $|m_{fi}|^2$, only involving detectors' internal structure, and the response function F, describing the interaction with the field, such that

$$F(\Delta E,\chi,t_i,t_f) = \int_{t_i}^{t_f} dt dt' G^+(t,t')\frac{d\tau}{dt}\frac{d\tau'}{dt'}e^{[-i\Delta E(\tau-\tau')]}\chi(\tau)\chi(\tau'), \tag{4.11}$$

where $G^+(x,x') = \langle 0|\phi(x)\phi(x')|0\rangle$ is the positive Wightman function, and τ' and the primed coordinates refer to the time t', while τ and the non-primed coordinates refer to the time t. With the above definitions, the probability of transition between two arbitrary states is given by

$$P_{|0\rangle;i\to f} = \lambda^2 |m_{fi}|^2 F(\Delta E, \chi, t_i, t_f). \tag{4.12}$$

Let us make some simplifications to re-obtain a well-known result. Taking $\chi = 1$, $t_i \to -\infty$ and $t_f \to +\infty$, and changing the variables of integration in (4.11), from t and t' to τ and $\Delta\tau := \tau - \tau'$ [30], we get

$$F(\Delta E) = \int_{-\infty}^{\infty} d\tau \int_{-\infty}^{\infty} d(\Delta\tau)\; G^+(\Delta\tau)\; e^{-i\Delta E\,\Delta\tau}. \tag{4.13}$$

This is a widely known result in the literature of particle detectors ([21, 22]), which says that the response function, and then also the probability of transition, is proportional to the Fourier transform of the positive Wightman function, as long as we can write it as $G^+(\Delta\tau)$.

4.2 TWO DETECTORS

Now, let us discuss the theory for two Unruh-DeWitt detectors, and finally apply it to rotating frames. The developments in this section are similar to the ones in section 3 of reference [63]. The total Hamiltonian and the free Hamiltonian of the field are still given by (4.1) and (4.3), respectively. With $|g_j\rangle$ and $|e_j\rangle$ being respectively the ground state and the excited state of the j-th detector, the two detectors free Hamiltonian is now given by

$$H_d = \frac{E}{2}\left[S_1^z \otimes \mathbb{1}_2 + \mathbb{1}_1 \otimes S_2^z\right] + \Omega(S_1^+ S_2^- + S_1^- S_2^+), \tag{4.14}$$

where $S_j^z = |e_j\rangle\langle e_j| - |g_j\rangle\langle g_j|$, $S_j^+ = |e_j\rangle\langle g_j|$ and $S_j^- = |g_j\rangle\langle e_j|$, for j = 1, 2. The operator multiplying Ω is a dipole interaction between detectors. Using Bell (maximally entangled) states, the above Hamiltonian can be diagonalized [13]. The four eigenstates are given by

$$|g\rangle = |g_1\rangle|g_2\rangle; \tag{4.15}$$

$$|a\rangle = \frac{1}{\sqrt{2}}\left(|g_1\rangle|e_2\rangle - |e_1\rangle|g_2\rangle\right); \tag{4.16}$$

$$|s\rangle = \frac{1}{\sqrt{2}}\left(|g_1\rangle|e_2\rangle + |e_1\rangle|g_2\rangle\right); \tag{4.17}$$

$$|e\rangle = |e_1\rangle|e_2\rangle, \tag{4.18}$$

with eigenvalues $-E$, $-\Omega$, $+\Omega$ and $+E$, respectively. A tensor product is implicit in the above notation. The ground state of both detectors is denoted as $|g\rangle$, $|s\rangle$ and $|a\rangle$ are the symmetric and anti-symmetric Bell states, respectively, and $|e\rangle$ denotes the state where both detectors are excited. Now, the interaction Hamiltonian is written as

$$H_{int}(t) = \lambda \sum_{j=1}^{2} \chi_j(\tau_j(t))\, m^{(j)}(\tau_j(t))\, \phi(x^\mu(\tau_j(t)))\, \frac{d\tau_j(t)}{dt}, \tag{4.19}$$

where λ is again the dimensionless coupling constant of the interaction, χ is the real-valued switch-function for the interaction of the detectors with the scalar field, and $m^{(j)}(\tau_j(t))$ is the monopole operator of the j-th detector. The field $\phi(x^\mu(\tau_j))$ is evaluated in the classical trajectory of each of the detectors, and the factor $d\tau_j/dt$ is the Jacobian to correct the time integration. The operators, $m^{(1)}(0)$ and $m^{(2)}(0)$, for two detectors in the basis $\{|g\rangle, |s\rangle, |a\rangle, |e\rangle\}$ are

$$m^{(1)}(0) = m(0) \otimes \mathbb{1} = \frac{1}{\sqrt{2}} \begin{bmatrix} 0 & m & m & 0 \\ m & 0 & 0 & m \\ m & 0 & 0 & -m \\ 0 & m & -m & 0 \end{bmatrix}, \tag{4.20}$$

$$m^{(2)}(0) = \mathbb{1} \otimes m(0) = \frac{1}{\sqrt{2}} \begin{bmatrix} 0 & m & -m & 0 \\ m & 0 & 0 & m \\ -m & 0 & 0 & m \\ 0 & m & m & 0 \end{bmatrix}. \tag{4.21}$$

In the interaction picture, for arbitrary initial and final states $|i\rangle$ and $|f\rangle$ of the detectors, respectively, we have

$$\langle f|m^{(j)}(\tau_j)|i\rangle = e^{i(E_f - E_i)\tau_j'} \langle f|m^{(j)}(0)|i\rangle = e^{i(E_f - E_i)\tau_j} m_{fi}^{(j)}. \tag{4.22}$$

where E_i and E_f are the energies of the initial and final detector states, respectively. The only possible transitions are the ones shown in figure 4.1, where both $m_{fi}^{(j)} \neq 0$. For simplicity, we take $\Omega = 0$, such that the Bell states are degenerated. The energy levels are also illustrated in figure 4.1.

To calculate the probability of transition between arbitrary states, we again use (4.7), the Schrödinger equation in the interaction picture, solved to first order as

$$\begin{aligned} U(t, t_i) &= \mathcal{T}\left\{\exp\left(-i\int_{t_i}^{t} H_{int}(t')dt'\right)\right\} = \\ U(t, t_i) &= 1 - i\lambda \int_{t_i}^{t_f} dt H_{int}(t) + \mathcal{O}(\lambda^2). \end{aligned} \tag{4.23}$$

Again, t_i is an arbitrary initial time, and $\mathcal{T}$ is the usual time-ordering operator. With the evolution operator, one can proceed with the steps in previous section to compute the probability of transition between arbitrary states $|i\rangle$ and $|f\rangle$ of the detectors, as

$$\begin{aligned} P_{|0_R\rangle;i\to f}(t_f, t_i) = \lambda^2 \int_{t_i}^{t_f} dt dt' \sum_{j,k=1}^{2} m_{fi}^{(j)*} m_{fi}^{(k)} \frac{d\tau_j(t)}{dt} \frac{d\tau_k(t')}{dt'} \chi(\tau_j)\chi(\tau_k) \\ \times \langle 0_R|\phi(x_j^\mu(\tau_j(t)))\phi(x_k'^\mu(\tau_k(t')))|0_R\rangle e^{-i(E_f - E_i)(\tau_j - \tau_k)}, \end{aligned} \tag{4.24}$$

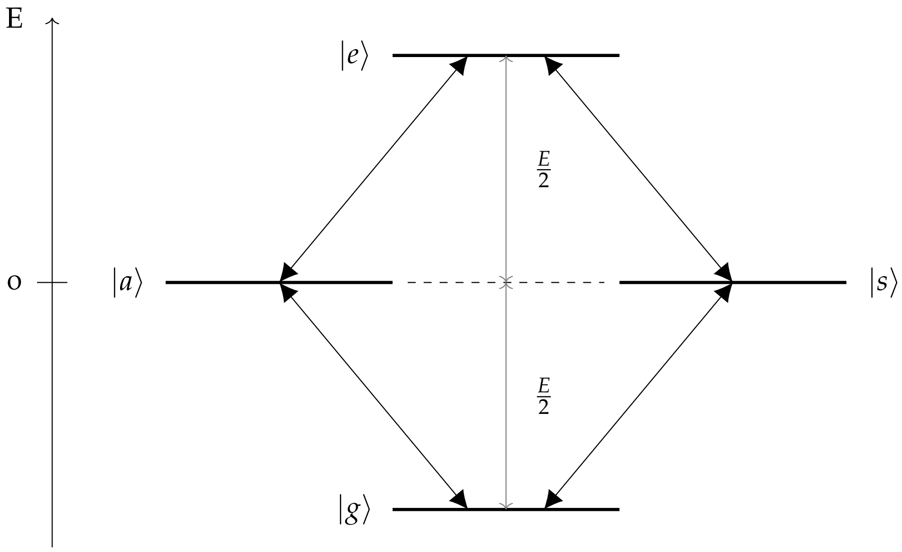

Figure 4.1: Energy levels and possible transitions between the eigenstates of the detectors' Hamiltonian (4.14), with Ω = 0. Adapted from Ficek et al [13].

where j and k label both detectors. Now there are four selectivity factors, $m_{fi}^{(j)*}m_{fi}^{(k)}$, and four response function, as follows:

$$F_{jk}(\Delta E,\chi,t_i,t_f) = \int_{t_i}^{t_f} dt \int_{t_i}^{t_f} dt' G^+_{jk}(t,t') \frac{d\tau_j(t)}{dt}\frac{d\tau_k(t')}{dt'} \times$$
$$\exp\left[-i\Delta E(\tau_j-\tau_k) + im(\varphi_j-\varphi_k) + ik(z_j-z_k)\right]\chi(\tau_j)\chi(\tau_k), \tag{4.25}$$

where $G^+_{jk}(x_j,x'_k) = \langle 0_R|\phi(x_j)\phi(x'_k)|0_R\rangle$ are the four positive Wightman functions. With the above definitions the probability of transition between two arbitrary states is given by

$$P_{|0_R\rangle;i\to f} = \lambda^2 \sum_{j,k=1}^{2} m_{fi}^{(j)*}m_{fi}^{(k)} F_{jk}(\Delta E,\chi,t_i,t_f). \tag{4.26}$$

From now, we will apply the theory of detectors to two Unruh-DeWitt detectors in a rotating frame, generalizing the results obtained by Cai, Li and Ren [68]. See also reference [29] for a rotating Unruh-DeWitt detector under non-equilibrium conditions and reference [69] for a discussion of a finite-time response function. To simplify our computations, we can use $z_1 = z_2$ and $\varphi_1 = \varphi_2$. From chapter 2, we get the proper times $\tau_j = \left(1 - w^2 r_j^2\right)^{1/2} t = t/\gamma_j$. The terms $d\tau_j/dt$ are constant in a circular motion, and can be factored out of time integrals. Now, using equation (3.61), into the response function, we get:

$$F_{jk} = \int_{t_i}^{t_f} dt dt' \sum_{\substack{m=-\infty,\\ n=1}}^{\infty} \int_{-\infty}^{\infty} dk \frac{J_m(k_{mn}r_j)J_m(k_{mn}r_k)e^{-i(\Delta E+\varepsilon)(\tau_j-\tau'_k)}}{4\pi^2 a^2 \gamma_j\gamma_k [J'_m(k_{mn}a)]^2 N^2_{kmn}}. \tag{4.27}$$

Let us change variables of integration from t and t' to t and $\Delta t = t - t'$. The modulus of the Jacobian for this coordinate transformation is one. Let us define $\Delta \bar{E} = \Delta E(1/\gamma_j - 1/\gamma_k)$ and $\Delta E' = \Delta E/\gamma_k$, and rewrite the exponential argument as follows:

$$\exp\left[-i\varepsilon(t-t') - i\Delta E\left(\frac{t}{\gamma_j} - \frac{t'}{\gamma_k}\right)\right] = \exp\left[-i(\varepsilon + \Delta E')(t-t') - i\Delta\bar{E}t\right]. \tag{4.28}$$

We will work with the asymptotic limits $t_i \to -\infty$ and $t_f \to \infty$.

Now, the response function per unit time t, the rate $R_{jk}(t) = \partial F_{jk}/\partial t$ can be computed

$$\begin{aligned} R_{jk} &= e^{-i\Delta\bar{E}t}\int_{-\infty}^{\infty} d(\Delta t) e^{-i(\Delta t)(\varepsilon+\Delta E')}\sum_{m,n}\int_{-\infty}^{\infty} dk \frac{J_m(k_{mn}r_j)J_m(k_{mn}r_k)}{4\pi^2 a^2\gamma_j\gamma_k[J'_m(k_{mn}a)]^2 N^2_{kmn}} \\ &= e^{-i\Delta\bar{E}t}\left[2\pi\delta(\varepsilon+\Delta E')\right]\sum_{m,n}\int_{-\infty}^{\infty} dk \frac{J_m(k_{mn}r_j)J_m(k_{mn}r_k)}{4\pi^2 a^2\gamma_j\gamma_k[J'_m(k_{mn}a)]^2 N^2_{kmn}}, \end{aligned} \tag{4.29}$$

where the delta function on the last equality was obtained by performing the integral on Δt, resulting in a factor $\delta[\Delta E' + (\sqrt{k^2 + k^2_{mn} + \mu^2} - m\omega)]$ after substituting ε.

The roots of the Bessel function are such that $\alpha_{mn} > m$, so, as $\omega a \leq 1$, the argument of the delta function is always positive, and the corresponding response function will be zero [30]. We will have non-zero response function and non-zero contribution to the transition rate if and only if $\Delta E' \leq 0 \leq m\omega - \sqrt{k^2_{mn} + \mu^2}$. This means that there is no excitation of an inertial detector in the rotating vacuum, it can only de-excite. It is consistent with the fact that all Bogoliubov's β coefficients are zero between the rotating and inertial modes. So inertial detectors can not detect particles in the rotating vacuum.

Assuming that $\Delta E' \leq m\omega - \sqrt{k^2_{mn} + \mu^2}$, we can expand the delta function in its roots, $\delta\big(f(k)\big) = \sum_{i-th\ root}\left(\frac{\delta(k-k_i)}{|f'(k_i)|}\right)$, with

$$f'(k) = \frac{k}{\sqrt{k^2 + k^2_{mn} + \mu^2}} = \frac{\sqrt{(m\omega - \Delta E')^2 - k^2_{mn} - \mu^2}}{m\omega - \Delta E'}. \tag{4.30}$$

Integrating the expanded delta function, the response function becomes:

$$\begin{aligned} R_{jk} &= \frac{e^{-i\Delta\bar{E}t}}{2\pi a^2\gamma_j\gamma_k}\sum_{m,n}\frac{J_m(k_{mn}r_j)J_m(k_{mn}r_k)|m\omega - \Delta E'|}{[J_{m+1}(k_{mn}a)]^2 N^2_{kmn}\sqrt{|(m\omega-\Delta E')^2 - k^2_{mn} - \mu^2|}} \\ &\to R_{jk} =: e^{-i\Delta\bar{E}t}C_{jk}, \end{aligned} \tag{4.31}$$

where we defined the numerical factor C_{jk} as all the terms in the above equation that does not depend on the time t. In the following, we show that R_{jk} is real, as expected. This will be discussed later.

We can express, in first-order perturbation theory, the transition rate $\dot{P} = dP/dt$ as

$$\Gamma_{|i\rangle \to |f\rangle} = \dot{P}_{|i\rangle \to |f\rangle} = \lambda^2 \sum_{j,k=1}^{2} m_{fi}^{(j)*} m_{fi}^{(k)} R_{jk}. \tag{4.32}$$

If we compute the C_{jk} numerical factor, we are able to study the allowed radiative processes in this system and its transition rates. But this factor is not fully determined yet in (4.31), we still need to specify the normalization used. We will compute it using both possible normalizations N_{kmn} (3.54) discussed in the previous section, for which the factor C_{jk} reads:

$K = \partial_T$:

$$C_{T_{jk}} = \frac{1}{\gamma_j \gamma_k} \sum_{m,n} \frac{J_m(k_{mn} r_j) J_m(k_{mn} r_k) \Theta[m\omega - \sqrt{k_{mn}^2 + \mu^2} - \Delta E']}{2\pi a^2 [J_{m+1}(k_{mn} a)]^2 \sqrt{(m\omega - \Delta E')^2 - k_{mn}^2 - \mu^2}}. \tag{4.33}$$

$K = \partial_t$:

$$C_{t_{jk}} = \frac{1}{\gamma_j \gamma_k} \sum_{m,n} \frac{J_m(k_{mn} r_j) J_m(k_{mn} r_k) |m\omega - \Delta E'| \Theta[m\omega - \sqrt{k_{mn}^2 + \mu^2} - \Delta E']}{2\pi a^2 [J_{m+1}(k_{mn} a)]^2 (-\Delta E') \sqrt{(m\omega - \Delta E')^2 - k_{mn}^2 - \mu^2}}. \tag{4.34}$$

5 ANALYSIS OF THE RADIATIVE PROCESSES

The discussion in this chapter is an identical transcription of section 4 of reference [63]. In this chapter, we will discuss the radiative processes of two Unruh-DeWitt detectors in a rotating frame. Our objective is to analyze and numerically calculate the transition rates for different initial conditions, stressing the relevance of each parameter. The stability of entangled states and the effects of entanglement harvesting and entanglement degradation are also discussed. For a more complete approach to tackle entanglement dynamics, we refer the reader to [70].

5.1 DISCUSSION OF THE RESPONSE FUNCTION

The response function presented in equations (4.33) and (4.34) is a product of the integral of an oscillatory term in t with a numerical factor called C_{jk}. Defining the rate $R_{jk}(t)$ as usual, being the derivative $dF_{jk}(t)/dt$ of the response function, the first term becomes only a phase. Notice that the phase $\Delta\bar{E}\,t = 0$ for both R_{11} and R_{22}, such that these terms will never become negative when calculating the transition rate Γ, as $\Delta\bar{E} = \Delta E(1/\gamma_j - 1/\gamma_k)$. The phase of the crossed terms, R_{12} and R_{21}, are complex conjugates, so, when summed, they will only result in a real factor times a trivial oscillatory term. In fact, there is no origin defined for the time coordinate, so we can specify it stating that we are performing the calculations to $t = 0$, which is equivalent to taking the absolute value of each R_{jk}.

It is worth to note that, when we changed variables in equation (4.28), we chose the time t of the first detector as the variable for the response function. We could have chosen the time t' of the second detector, and the only effect would be that $\Delta E'$ would be equal to $\Delta E/\gamma_j$ instead of $\Delta E/\gamma_k$. That is, the choice of the time coordinate to describe the system only implies in which gamma factor will Doppler shift the gap of the detector in our description of the system.

We have two possible Killing vectors defining our internal product, ∂_T and ∂_t, being the generator of temporal displacements in the non-rotating and in the rotating frames, respectively. Using suitable boundary conditions, both are time-like in all of the radially-bounded spacetime. The difference between those normalizations is given by a term $|m\omega - \Delta E'|/|\Delta E'| = |1 - m\omega/\Delta E'|$ inside the sums. It can only be significant for $m\omega \approx \Delta E'$. According to the convergence criterion described in the next subsection, we always had $m_{max} \leq 200$, so we need $\omega \approx 0.1$ for this term to be relevant. We will call it a “non-relativistic regime" when $\omega \ll 0.1$, and a “relativistic regime" otherwise. In fact, when we compare the numerical results for the transition rates, we confirm the values of the transition rates with both normalizations begin to differ only in the relativistic regime, but none of the qualitative features will differ between them (cf. figure 5.2).

Despite having eight possible transitions shown in figure 4.1, we will find that we have only three different transition rates. The first one is related to de-excitations involving the symmetric entangled state $\left(\Gamma_{|e\rangle\to|s\rangle} = \Gamma_{|s\rangle\to|g\rangle}\right)$; the second, to de-excitations involving the antisymmetric entangled state $\left(\Gamma_{|e\rangle\to|a\rangle} = \Gamma_{|a\rangle\to|g\rangle}\rangle\right)$, and, lastly, the third one, involving any excitation $\left(\Gamma_{|g\rangle\to|s\rangle} = \Gamma_{|s\rangle\to|e\rangle} = \Gamma_{|g\rangle\to|a\rangle} = \Gamma_{|a\rangle\to|e\rangle}\right)$. As any of the possible transitions necessarily involve one pure state and one entangled state, any of them by themselves represent either entanglement degradation or entanglement harvesting.

In order to compute transition rates, we have to combine the rates (individual rates R_{11} and R_{22} and crossed rates R_{12} and R_{21}) with the selectivity factors. Both kinds of response functions have sums of products of Bessel cylindrical functions, which have strong oscillatory behavior. The individual rates show products of those functions taken at the same point, so, as they are squared, these terms will never be negative. Only the crossed rates can be negative. Therefore, when we take both detectors to the same radial coordinate, $r_1 = r_2$, the crossed response functions will also be necessarily positive. It is expected that in this situation we would get at least a local maximum in the transition rate, for any equal radial coordinates. We found it to be evidently a global maximum in all explicitly calculated cases, and one of them is exhibited in the next subsection. This behavior has been widely discussed in the literature [71]. When the detectors are too close, they interfere stronger with each other. In fact, as we will see (cf. figure 5.1), the crossed response functions is only significantly different from zero when $r_1 \approx r_2$.

Due to the dependence $1/\sqrt{(m\omega - \Delta E')^2 - k_{mn}^2 - \mu^2}$ in the response function, divergences can appear. In the next subsection, we see them clearly as peaks in the plot of the transition rate by ωa when it approaches one, as we see in figure 5.6(c), with $|\Delta E|a = 200$. Analyzing the denominator of C_{jk}, we see that these singularities only happen when $m\omega \approx \Delta E' \to ma\omega \approx |\Delta E'|a$, or when $k_{mn} \approx \Delta E' \to \alpha_{mn} \approx |\Delta E'|a$. Since in the sums m_{max} and $n_{max} < 200$, let us take $\alpha_{200,200}$ as superior limit for α_{mn}. We have $\alpha_{200,200} \approx 920 > 200$. So, for $|\Delta E'|a = 200$, we have m and n such that $\alpha_{mn} \approx |\Delta E'|a \approx ma\omega$. In this case, we will have singularities from both terms, in many of (m, n) pairs. If we had chosen a one order of magnitude bigger, we would not expect any singularity. If we fix a, but reduce ω, we will not have divergences caused by the factor $m\omega$, but we may still have some singularities coming from k_{mn}. Since the only place where μ appears is in this factor, we can say that its main effect is to change the regime when we start having singularities.

For $\gamma_1, \gamma_2 \approx 1$, we can go back into equation (4.33) and take the approximation $\Delta E' \approx \Delta E$, such that the only dependence on the radial coordinates will be in the Bessel functions. We will specify the details of this approximation for the normalization using the ∂_T Killing vector, but for ∂_t it would be basically the same, just including the factor $|1 - m\omega/\Delta E|$ in the normalization. We approximate the C_T-factor as

$$C_{T_{jk}} \approx \sum_{m,n} T_{mn} J_j^{mn} J_k^{mn}, \tag{5.1}$$

where

$$T_{mn} = \frac{\Theta[m\omega - \sqrt{k_{mn}^2 + \mu^2} - \Delta E]}{2\pi a^2 [J_{m+1}(k_{mn}a)]^2 \sqrt{(m\omega - \Delta E)^2 - k_{mn}^2 - \mu^2}} \tag{5.2}$$

and

$$J_j^{mn} = \frac{J_m(k_{mn} r_j)}{\gamma_j}. \tag{5.3}$$

Now, the rate can be written in a much simpler way. Using the matrix elements of (4.20) and (4.21) in equation (4.32), we get two main cases, transitions involving the symmetric entangled state, and transitions involving the anti-symmetric entangled state:

$$\begin{aligned}\Gamma'_{symm} &= \lambda^2 \sum_{m,n} T_{mn} (J_1^{mn} + J_2^{mn})^2; \\ \Gamma'_{anti-symm} &= \lambda^2 \sum_{m,n} T_{mn} (J_1^{mn} - J_2^{mn})^2,\end{aligned} \tag{5.4}$$

where the Γ' represents an approximated transition rate. It is clear, from these equations, that transition rates involving the anti-symmetric entangled state are zero when $r_1 = r_2$. Moreover, only for $r_1 = r_2$ we know that J_1^{mn} and J_2^{mn} have the same signal for all m's and n's. So, it can also be expected that this point is the maximum of transition rates involving the symmetric entangled state. In the next sub-section, we compare numerical analysis using the approximated transition rates in equation (5.4), and the ones calculated using the functions in equation (4.33).

5.2 NUMERICAL ANALYSIS OF RADIATIVE PROCESSES

This section is devoted to the study of numerical values for the transition rates of some interesting cases, revealing the behavior of the system. Our convergence criterion for the sums in m and n was that the relative difference between the following terms of the sum should be less than 10^{-7}, 10 times in a row. Although there are sums that do not converge for $m, n \leq 100$, for $m, n \leq 200$ all of them converged for the chosen parameters. All of the following plots have dimensionless quantities in both axes. Unless we explicitly say otherwise, the default values for the parameters are such that $|\Delta E|a = 20000$, $a\omega = 1$, $\mu/|\Delta E| = 0.035$ and $\Delta E = -20$ (in arbitrary units of energy). For simplicity, we also took $\lambda = 1$, and the monopole operator constant $m^{(1)} = m^{(2)} = \sqrt{2}$.

First, let us study the behavior of the individual terms C_{11} and C_{22} as a function of r_2. There is no dependence on r_2 in C_{11}, so it will be a constant. The C_{22} term is shown in figure 5.1(b), and it has a Bessel dependence on r_2, but it is always squared, so it can never be negative. The crossed terms C_{12} and C_{21}, on the other hand, has the argument of only one of the Bessel functions varying with r_2. As this function has an oscillatory behavior, we also expect the crossed C factors to be oscillatory, as in figures 5.1(c) and 5.1(d). They should have a local (at least) maximum when $r_1 = r_2$ because that's the only point where all the terms in the m and n sums are positive.

Although its difficult to infer the main properties the transition rate Γ, in section 4.1 we make an approximation ($\gamma_1 \approx \gamma_2 \approx 1$) to make its behavior more clear and to conclude the existence of a global maximum or a global minimum in the symmetric and anti-symmetric transitions, respectively. This happens because, in the computation of the transition rate, C_{11} and C_{22} are always positive, however, the crossed terms C_{12} and C_{21} contributes positively for transitions involving the symmetric state and negatively for transitions involving the anti-symmetric state. In fact, we see in figures 5.4 and 5.7 that there is a global maximum for transitions involving the symmetric entangled state, and a global minimum for transitions involving the anti-symmetric entangled state.

Now, let us calculate the transition rates of the system. First, we need to discuss the normalization used in these calculations. The physical meaning of this choice is the time-like Killing vector used to quantize the massive scalar field, giving the two different normalizations in equation (3.54). As discussed in subsection 5.1, they only differ by a factor $|1 - m\omega/\Delta E'|$, which in general is very close to one. In figure 5.2 we show the transition rate from $|s\rangle$ to $|g\rangle$ as a function of r_2, calculated with both normalizations. We can see that they begin to visually differ for $r_2/a > 0.1$, but there is no qualitative relevant difference. So, in the discussions concerning the dependence on other parameters, we will omit plots using ∂_t as the Killing vector, since they will not provide any further information.

Besides that, we can calculate the transitions using the equation (4.34) for the C_T's and plugging into the transition rate, or by using directly (5.4). In figure 5.3, we compare a de-excitation involving the symmetric entangled state computed in both ways, with or without the approximation, respectively. In the non-relativistic regime, the

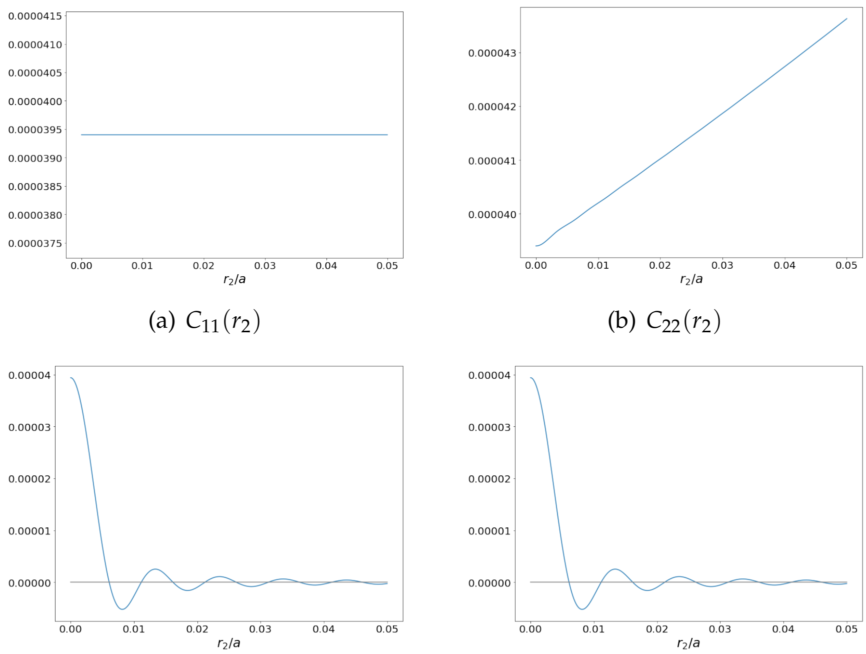

(a) $C_{11}(r_2)$ (b) $C_{22}(r_2)$

(c) $C_{12}(r_2)$ (d) $C_{21}(r_2)$

Figure 5.1: Individual C_{jk} factors as a function of r_2, using ∂_T to define the normalization. Figures (a) and (b) are the numerical factors of the individual response functions of the first and second detectors, respectively. Figures (c) and (d) are the numerical factors of the crossed response functions F_{12} and F_{21}, respectively. Here, $r_1/a = 0$, $|\Delta E|a = 20000$, $a\omega = 1$, $\mu/|\Delta E| = 0.035$ and $\Delta E = -20$ in arbitrary units of energy.

graphs are visually identical, but, in the relativistic one, we see that they differ significantly. It was also expected that the peaks were to change, since we also changed the denominator, ignoring a γ factor, to get in (5.4).

Let us analyze the different possible transitions and transition rates. We will first study the de-excitations involving the symmetric entangled state. Now, using figure 5.4, we compare the rate as a function of r_2 in two different situations, when r_1 is in or out of the origin, respectively. As expected by the discussion in subsection 5.1 and by the individual terms in figure 5.1, in both cases we have a maximum when $r_1 = r_2$.

The behavior of the rate from figure 5.4(a) is very similar to other situations studied in the literature [71], with the response function oscillating, with a large amplitude only in the first few oscillations. In our problem, the response function does not go to zero when r_2 increases. This behavior could be expected since the "gravitational field" increases at larger distances [72]. Even that the detectors get far away from each other, we still have a growing effect of the "gravitational field" affecting the system.

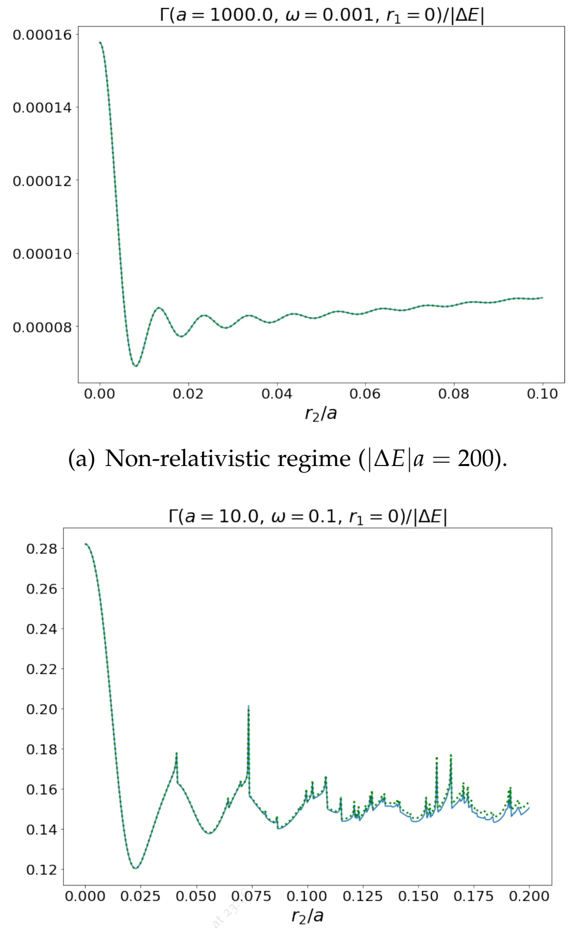

(a) Non-relativistic regime ($|\Delta E|a = 200$).

(b) Relativistic regime ($|\Delta E|a = 200$).

Figure 5.2: Transition rate involving the symmetric entangled state calculated for different normalization constants, as a function of r_2. The continuous blue graph was computed using the ∂_T Killing vector, and the dotted green graph was computed using the ∂_t one. The first graph shows the non-relativistic regime, and the second one shows the relativistic regime. In both cases, $r_1/a = 0$, $a\omega = 1$, $\mu/|\Delta E| = 0.035$ and $\Delta E = -20$ in arbitrary units of energy.

Let us discuss the dependence in ω in a non-relativistic regime of the system, fixing $|\Delta E|a = 20000$. With other parameters having the same values as in the previous analysis, and now fixing $r_1 = 0$ and $r_2/a = 0.1$, we will take small values of ω, as shown in figure 5.5. All the three graphs gives us the same normalized (and very small) transition rate between 8×10^{-5} and 9×10^{-5}, coinciding with the value for $r_2/a = 0.1$ in figure 5.4(a). Taking $a\omega \leq 10^{-2}$ and 1, the fluctuations in the rate when ω changes are respectively 7 and 3 orders of magnitude smaller than the actual value of the rate. So, in this regime, changing ω basically does not change the rate.

Now, let us discuss the same dependence in a relativistic regime. Let us fix $|\Delta E|a = 200$, keeping $r_1 = 0$ and $r_2/a = 0.1$. In this case,

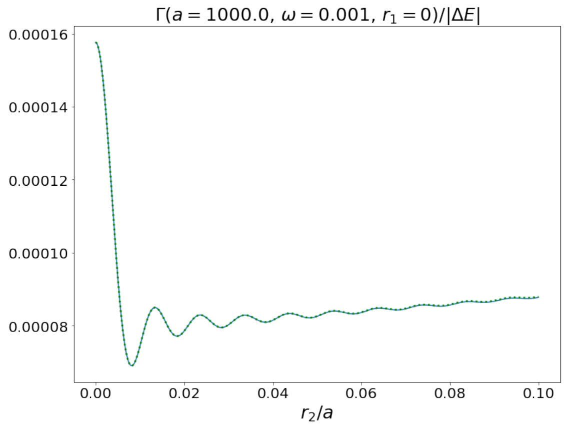

(a) Non-Relativistic regime ($|\Delta E|a = 20000$).

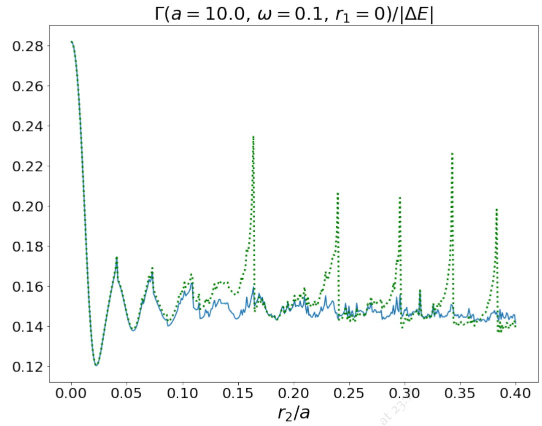

(b) Relativistic regime ($|\Delta E|a = 200$).

Figure 5.3: Comparison between the transition rates of a de-excitation involving the symmetric entangled state calculated from C_T, or using the approximation Γ'_{symm}. In each graph, the first one is the continuous blue line, and the second one is the dotted green graph. The first graph presents the non-relativistic regime, and the second one presents the relativistic regime. In both cases, $r_1/a = 0$, $a\omega = 1$, $\mu/|\Delta E| = 0.035$ and $\Delta E = -20$ in arbitrary units of energy.

we can see in figure 5.6 that both the rate and its fluctuations are way more relevant than in the non-relativistic one. There are a lot of discontinuities in those graphs as we take $|\Delta E|a = 200$ and $a\omega$ closer to one, since we approach the singularities discussed in subsection 5.1, annihilating the denominator $|(m\omega - \Delta E')^2 - k_{mn}^2 - \mu^2|^{1/2}$. But, except for those discontinuities, the dimensionless transition rate does not change significantly with the value of ω when we fix the other parameters. In the non-relativistic case, with $|\Delta E|a = 20000$, it was roughly 9×10^{-5}. In the relativistic case, with $|\Delta E|a = 200$, excluding discontinuities, it is always between 0.15 and 0.16.

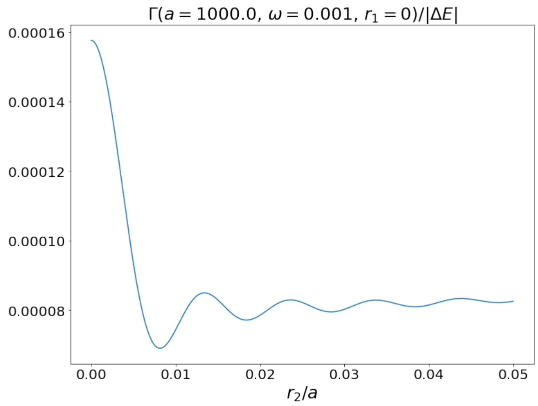

(a) $r_1/a = 0$

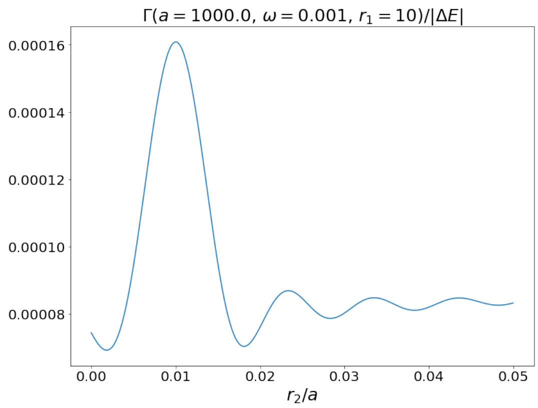

(b) $r_1/a = 0.01$

Figure 5.4: Symmetric de-excitation rates for the non-relativistic regime. In the first graph, the first detector is fixed in the origin. In the second graph, the first detector is also fixed, but out of the origin. In both cases, $|\Delta E|a = 20000$, $a\omega = 1$, $\mu/|\Delta E| = 0.035$ and $\Delta E = -20$ in arbitrary units of energy.

We can also see, from equations (4.33) and (4.34), that the only significance of the mass of the field, μ, is to change the relativistic regime, changing the zeros of the denominator of the response function.

There is also the de-excitations that involve the anti-symmetric entangled state. In figure 5.7, we show the behavior of the transition rate for this case when the first detector is in the origin or out of the origin, respectively. In figure 5.8, we show graphs of this transitions computed from the function C_T, or from the approximation $\Gamma'_{anti-symm}$. As in the symmetric de-excitation case, the approximation is very good for the non-relativistic regime but very different from the actual transition rate for the relativistic one.

Notice that in figure 5.7 the anti-symmetric transition rate vanishes for $r_1 = r_2$. In fact, we could think of an intuitive argument for understanding this behavior. The only parameter that differs both detectors in this model is the distance from the origin. If we take

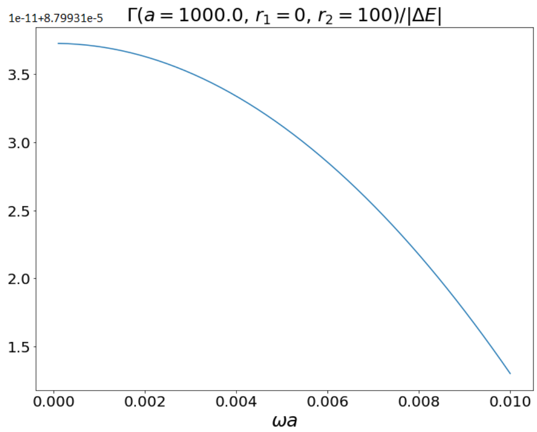

(a) $10^{-4} \leq \omega a \leq 10^{-2}$.

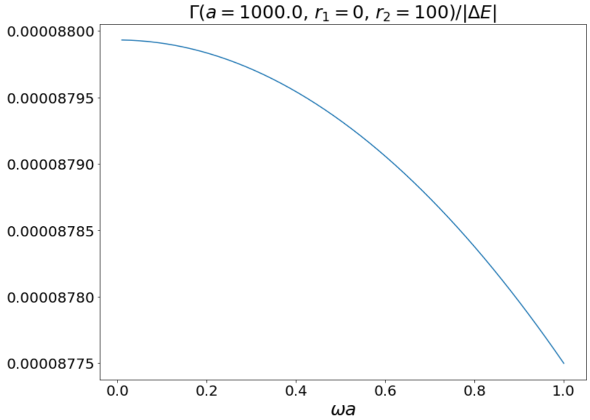

(b) $10^{-2} \leq \omega a \leq 1$.

Figure 5.5: Dependence of the transition rate as a function of ω, for a fixed, in the non-relativistic regime ($|\Delta E|a = 20000$). The first graph shows the interval $10^{-4} \leq \omega a \leq 10^{-2}$, and the second graph shows the interval $10^{-2} \leq \omega a \leq 1$. In both cases, $r_1/a = 0$, $r_2/a = 0.1$, $\mu/|\Delta E| = 0.035$ and $\Delta E = -20$ in arbitrary units of energy.

equal radii, there are no physical means of distinguishing them. If we interchange both detectors, we do not expect anything to happen to the state. But, in the anti-symmetric entangled state, the system's state should be anti-symmetric if we exchange both detectors. So, it seems not to be possible to have a transition from the excited state to the anti-symmetric entangled state when $r_1 = r_2$.

Now, for r_1 very different from r_2, the symmetric and anti-symmetric cases should have very similar transition rates, because the crossed response functions becomes very small, as seen in figures 5.1(c) and 5.1(d). In figure 5.9 we explicitly compare the transition rates of de-excitations involving the symmetric and the anti-symmetric entangled states for $r_1/a = 0.01$, and r_2/a varying. Both functions goes to the same value near 8×10^{-5} as $r_2 \gg r_1$, with the same behavior.

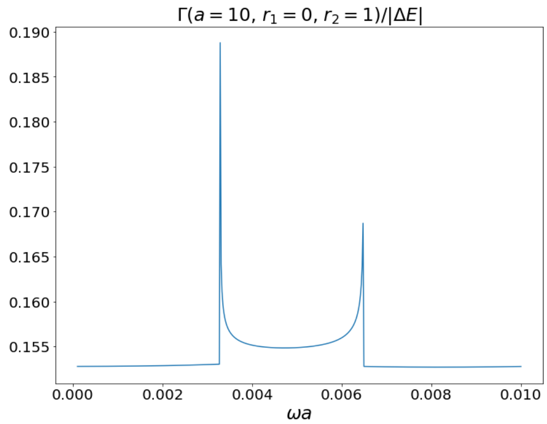

(a) $10^{-4} \leq \omega a \leq 10^{-2}$.

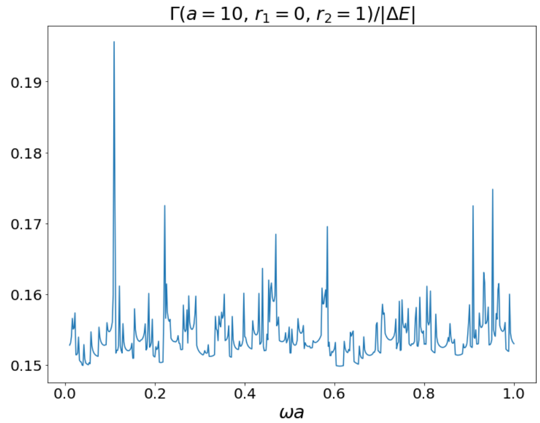

(b) $10^{-2} \leq \omega a \leq 1$.

Figure 5.6: Dependence of the transition rate as a function of ω, for a fixed, in the relativistic regime ($|\Delta E|a = 200$). The first graph shows the interval $10^{-4} \leq \omega a \leq 10^{-2}$, and the second graph shows the interval $10^{-2} \leq \omega a \leq 1$. In both cases, $r_1/a = 0$, $r_2/a = 0.1$, $\mu/|\Delta E| = 0.035$ and $\Delta E = -20$ in arbitrary units of energy.

If both crossed rates, R_{12} and R_{21}, tend to zero, we have only transitions caused by the individual rates. It is expected that even decaying from $|e\rangle$, the final state would not be entangled. In fact, if we have the same transition rate for $|s\rangle$ and $|a\rangle$, with the same sign, we are just generating the pure state $|g\rangle_1 \otimes |e\rangle_2$. But, when $r_1 \approx r_2$, the transitions on the two cases are very different. While the symmetric case displayed a maximum, the anti-symmetric one will display a minimum. In fact, the last one is equal to zero in $r_1 = r_2$, as shown in figure 5.7. Graphs of anti-symmetric transition rates as a function of ω are visually identical to the graphs in figures 5.5 and 5.6, so they were omitted.

In section 4, we obtained that, for the response function to be different than zero, we needed $\Delta E < 0$. That means we can only see de-excitations in our system. It was already expected, as the rotating

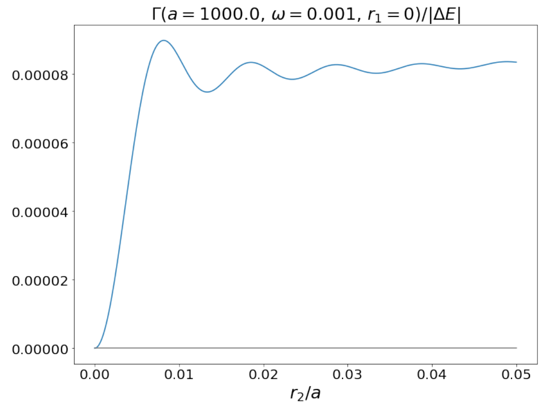

(a) $r_1/a = 0$

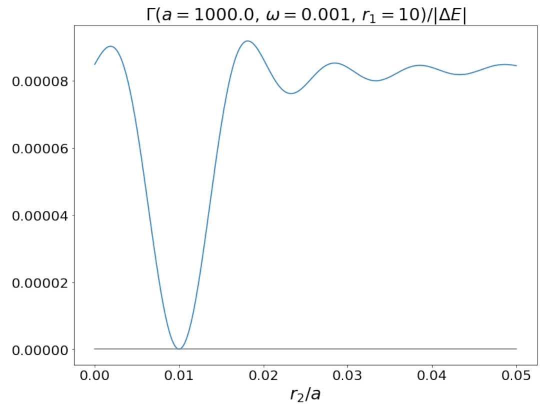

(b) $r_1/a = 0.01$

Figure 5.7: Anti-symmetric de-excitation rates for the non-relativistic regime. In the first graph, the first detector is fixed in the origin. In the second graph, the first detector is also fixed, but out of the origin. In both cases, $|\Delta E|a = 20000$, $\omega a = 1$, $\mu/|\Delta E| = 0.035$ and $\Delta E = -20$ in arbitrary units of energy.

vacuum was shown in section 3.3 to be equivalent to the Minkowski vacuum. So, we trivially get that all excitations are identical, and $\Gamma_{|g\rangle\to|s\rangle} = \Gamma_{|g\rangle\to|a\rangle} = \Gamma_{|s\rangle\to|e\rangle} = \Gamma_{|a\rangle\to|e\rangle} = 0$. But there is a more interesting behavior on the Γ's as a function of ΔE. In this discussion, we will take $r_1/a = 0$ different from $r_2/a = 0.1$, so there is no significant difference between transitions involving symmetric or anti-symmetric Bell states, as the crossed rates C_{12} and C_{21} are small compared to C_{11} and C_{22}. Let us use a transition involving the symmetric state. We can see in figure 5.10 that there is a gap where transitions are more probable to happen. When the energy of the gap is above some (negative) upper value, there is no transition at all. For negative energy gaps much bigger (in modulus) than $m\omega$, α_{mn}/a, and μ, it is expected that the transition rate goes to zero since the rate will be roughly proportional to $1/|\Delta E'|$. Between those limits, it oscillates around a function that steadily grows with the modulus $|\Delta E|$, with a

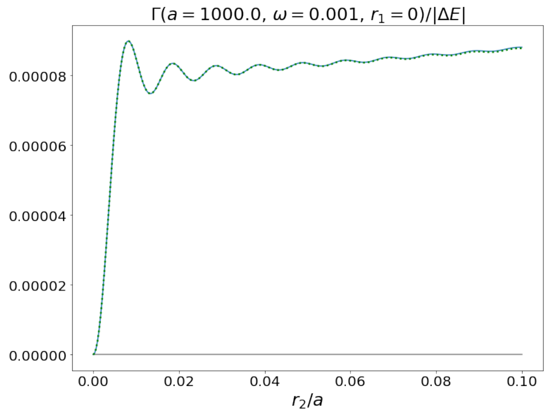

(a) Non-Relativistic regime.

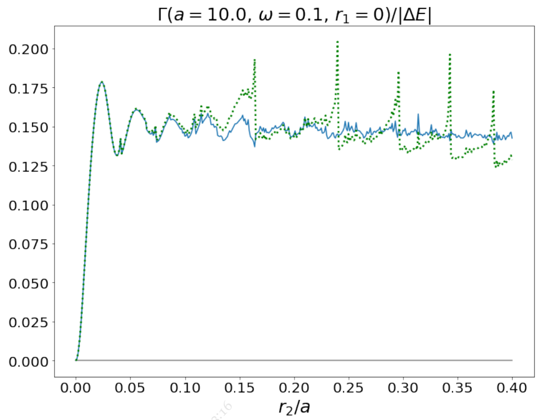

(b) Relativistic regime.

Figure 5.8: Comparison between the transition rates of a de-excitation involving the anti-symmetric entangled state calculated from C_T, or using the approximation Γ'_{symm}. In each graph, the first one is the continuous blue line, and the second one is the dotted green line. The first graph presents the non-relativistic regime ($|\Delta E|a = 20000$), and the second one presents the relativistic regime ($|\Delta E|a = 20$). In both cases, $\omega a = 1$, $\mu/|\Delta E| = 0.035$ and $\Delta E = -20$ in arbitrary units of energy.

behavior very similar to other works with rotating detectors (see, for example, [73]). The extremes of the oscillations depend on the radius a of boundary condition, as it defines the normal modes of the field that mediates the interaction. The asymptotic behavior of the transition rate as $1/|\Delta E'|$ when $\Delta E \to -\infty$ is illustrated in figure 5.10 by the green dots plotted, as a function $\propto 1/|\Delta E'|$.

We can try to define the extrema of the interval of ΔE where the transition rates oscillates by inspection of equation (4.33). The greater limit of the interval is a specific value defined by the Θ function, that requires $m\omega - \sqrt{k_{mn}^2 + \mu^2} - \Delta E' > 0$. So, for the other parameters fixed, ΔE_{max} for having a non-zero transition rate will be given by

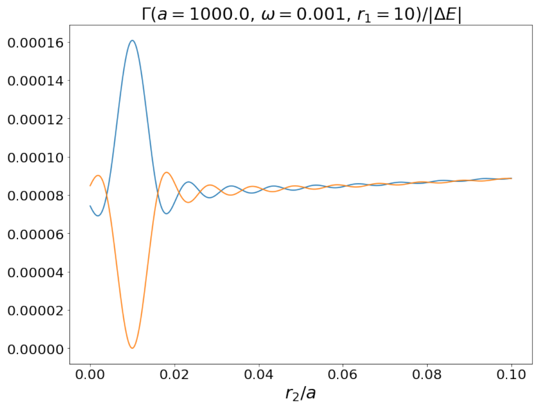

Figure 5.9: Comparison between transition rates for de-excitations involving the symmetric and the anti-symmetric states, respectively being the blue continuous line and the orange continuous line, as a function of r_2. This is the non-relativistic regime ($|\Delta E|a = 20000$), and the first detector is fixed in $r_1/a = 0.01$. Again, $\omega a = 1$, $\mu/|\Delta E| = 0.035$ and $\Delta E = -20$ in arbitrary units or energy.

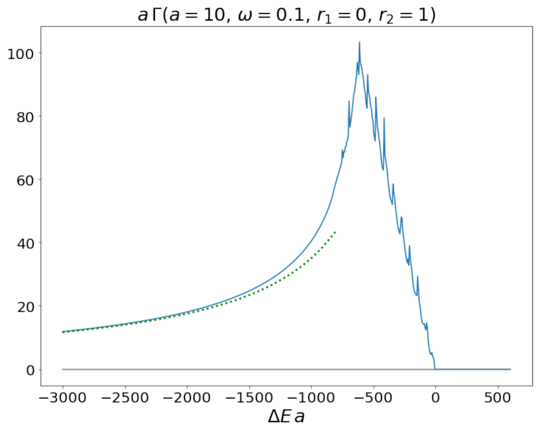

Figure 5.10: Dependence of the transition rate on the energy gap of the detector, for $a = 10$ (in arbitrary units of space). The green dotted plot refers to the asymptotic limit $\Delta E \to -\infty$, where the transition rate goes with $1/|\Delta E'|$. Here, $r_1/a = 0$, $r_2/a = 0.1$, $\omega a = 1$ and $\mu a = 7$.

$\Delta E_{max} = \gamma_2 \cdot \max_m(m\omega - \sqrt{k_{m1}^2 + \mu^2})$, already taking the maximum in n, for $n = 1$. The minimum value of the interval is related to the regime where Γ asymptotically behaves like $1/\Delta E$. That occurs when the term $(m\omega - \Delta E')^2 - k_{mn}^2 - \mu^2$ tends to $(\Delta E')^2$, that is, when $\Delta E \ll -\gamma_2 \cdot \max_m(m\omega, \alpha_{mn}/a, \mu)$.

So far we have computed transition rates between states of the system, and we used them to discuss, among other features, the stability of entangled states. A more direct way of analyzing it is to compute the mean life of those states. Since we have no excitation,

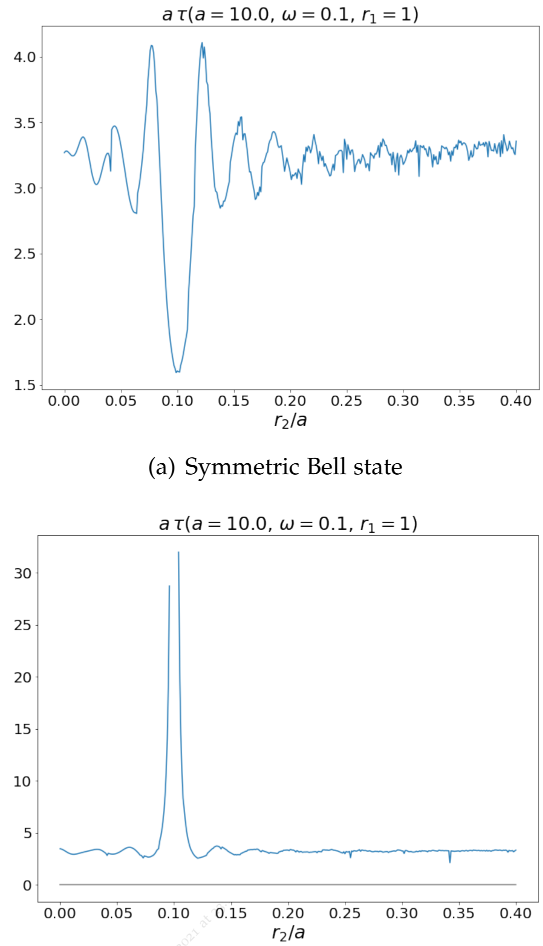

(a) Symmetric Bell state

(b) Anti-symmetric Bell state

Figure 5.11: The first and second graphs represent the mean-lifes of the symmetric and the anti-symmetric entangled Bell states, respectively, as a function of r_2, in the relativistic regime ($|\Delta E|a = 200$), with $\omega a = 1$, $\mu/|\Delta E| = 0.035$ and $\Delta E = -20$ in arbitrary units or energy.

entangled states can only decay to the ground state $|g\rangle$ of the system, so the mean life of an entangled state $|i\rangle$ is given by

$$\tau_{|i\rangle}(r_1, r_2; a, \omega, \Delta E, \mu) = [\Gamma_{|i\rangle \to |g\rangle}(r_1, r_2; a, \omega, \Delta E, \mu)]^{-1}. \quad (5.5)$$

In figure 5.11, the behavior of the mean life of both the symmetric and anti-symmetric entangled Bell states is presented. As already pointed out, we see that, for $r_1 = r_2$, the mean life of the symmetric entangled state is a minimum, and the mean life of the anti-symmetric one diverges, as this state becomes stable. For other values of r_2, we see the mean life oscillating, with several peaks, as we are in the relativistic regime, but its value is always between 3 and 3.5. As r_2 gets more different from r_1, the amplitudes of the oscillations become smaller. In the non-relativistic regime, the mean life would be a smooth function of r_2, since there are no peaks in the transition rate, and consequently no peaks in the mean life.

6 CONCLUSIONS

In this thesis, two entangled Unruh-DeWitt detectors coupled with a massive scalar field are studied. We discuss the radiative processes in a uniformly rotating frame, with Davies-Dray-Manogue's cylinder as the boundary condition for the field. Motivated by Davies et al [30] concerning rates in rotating frames, and by Rodriguez-Camargo et al [69] – entanglement of two detectors in a non-inertial frame (Rindler space-time, in that case) – radiative processes between two detectors in a rotating frame are discussed. Notice that the detectors are under the influence of different "gravitational fields".

For this objective, we made a historical review of relativistic rotation and discussed one of the approaches that could be compatible with Quantum Field Theory. In the sequence, we discussed Quantum Field Theory results that would be used in what follows, and we quantized a massive scalar field in a rotating frame, in a radially-bounded spacetime.

After discussing the basic theory of Unruh-DeWitt detectors, we show that there can not be any excitation of the detector system in this frame, extending the Davies et al. result for two entangled detectors. It is consistent with the Bogoliubov's β coefficients between Minkowski and the rotating field modes being zero. There is a non-zero crossed response function due to the coupling with the scalar field. This crossed term is responsible for transitions involving pure states and entangled states of both detectors. As we computed, only for $r_1 \approx r_2$ the crossed response functions are significantly different from zero, and this was important to study transitions involving entangled states. From the monopole matrices, we see that transition rates for de-excitations can be separated into two disjoint cases: the ones involving $|s\rangle$, and the ones involving $|a\rangle$. Specifically, $\Gamma_{|e\rangle \to |s\rangle} = \Gamma_{|s\rangle \to |g\rangle}$ and $\Gamma_{|e\rangle \to |a\rangle} = \Gamma_{|a\rangle \to |g\rangle}$. The second ones tend to zero when $r_2 \to r_1$, where the first ones have their maximum, as a consequence of the behavior of the crossed response functions.

The entanglement harvesting effect can only be seen for $r_1 \approx r_2$, and only in the de-excitation $|e\rangle \to |s\rangle$ between the state where both detectors are excited and the maximally entangled symmetric state. The crossed response function tends to zero for other values of radial coordinates, and the transitions to anti-symmetric and symmetric entangled states will have the same rate, generating a statistically pure state. On the other hand, entanglement degradation happens for both the transitions $|s\rangle \to |g\rangle$ and $|a\rangle \to |g\rangle$. The anti-symmetric entangled state is the only stable state, and only for $r_1 = r_2$, when the transition rate goes to zero. Mean-life of both entangled states are also studied. One can also look at the divergence in the mean-life plot for $r_1 = r_2$, in the anti-symmetric de-excitation, to verify the existence of a stable state. Finally, there are no entanglement effects associated with excitations, since there is no excitation at all.

The issues investigated in this thesis could be continued by studying the radiative processes of two detectors in the scenario of a non-time orthogonal metric, for instance, in the Kerr spacetime, where the effects over radiative processes can be analyzed. From this method, the possibility of extracting entanglement from a rotating black hole vacuum can be analyzed. One could also discuss the degradation of entangled states, comparing it with other works about entanglement dynamics in Kerr spacetimes [12]. Radiative processes with electromagnetic fields and entangled atoms can also be considered, as more realistic models. Moreover, the master equation approach could provide a more complete treatment for the dynamics of entangled detectors interacting with quantum fields.

BIBLIOGRAPHY

[1] Michael A. Nielsen and Isaac L. Chuang. *Quantum Computation and Quantum Information: 10th Anniversary Edition*. 10th. New York: Cambridge University Press, 2011.

[2] Jurgen Audretsch and Rainer Muller. "Spontaneous excitation of an accelerated atom: The Contributions of vacuum fluctuations and radiation reaction." In: *Phys. Rev.* A50 (1994), pp. 1755–1763. DOI: 10.1103/PhysRevA.50.1755. arXiv: gr-qc/9408019 [gr-qc].

[3] Asher Peres and Daniel R. Terno. "Quantum information and relativity theory." In: *Rev. Mod. Phys.* 76 (2004), pp. 93–123. DOI: 10.1103/RevModPhys.76.93. arXiv: quant-ph/0212023 [quant-ph].

[4] Greg L. Ver Steeg and Nicolas C. Menicucci. "Entangling power of an expanding universe." In: *Phys. Rev.* D79 (2009), p. 044027. DOI: 10.1103/PhysRevD.79.044027. arXiv: 0711.3066 [quant-ph].

[5] Jiawei Hu and Hongwei Yu. "Entanglement generation outside a Schwarzschild black hole and the Hawking effect." In: *JHEP* 08 (2011), p. 137. DOI: 10.1007/JHEP08(2011)137. arXiv: 1109.0335 [hep-th].

[6] Eduardo Martin-Martinez and Nicolas C. Menicucci. "Entanglement in curved spacetimes and cosmology." In: *Class. Quant. Grav.* 31.21 (2014), p. 214001. DOI: 10.1088/0264-9381/31/21/214001. arXiv: 1408.3420 [quant-ph].

[7] G. Menezes and N. F. Svaiter. "Vacuum fluctuations and radiation reaction in radiative processes of entangled states." In: *Phys. Rev.* A92.6 (2015), p. 062131. DOI: 10.1103/PhysRevA.92.062131. arXiv: 1508.04513 [hep-th].

[8] Jiawei Hu and Hongwei Yu. "Entanglement dynamics for uniformly accelerated two-level atoms." In: *Phys. Rev.* A91.1 (2015), p. 012327. DOI: 10.1103/PhysRevA.91.012327. arXiv: 1501.03321 [quant-ph].

[9] G. Menezes. "Radiative processes of two entangled atoms outside a Schwarzschild black hole." In: *Phys. Rev.* D94.10 (2016), p. 105008. DOI: 10.1103/PhysRevD.94.105008. arXiv: 1512.03636 [gr-qc].

[10] G. Menezes and N. F. Svaiter. "Radiative processes of uniformly accelerated entangled atoms." In: *Phys. Rev.* A93.5 (2016), p. 052117. DOI: 10.1103/PhysRevA.93.052117. arXiv: 1512.02886 [hep-th].

[11] G. Menezes. “Spontaneous excitation of an atom in a Kerr spacetime.” In: *Phys. Rev.* D95.6 (2017). [Erratum: Phys. Rev.D97,no.2,029901(2018)], p. 065015. DOI: 10.1103/PhysRevD.95.065015. arXiv: 1611.00056 [gr-qc].

[12] G. Menezes. “Entanglement dynamics in a Kerr spacetime.” In: *Phys. Rev.* D97.8 (2018), p. 085021. DOI: 10.1103/PhysRevD.97.085021. arXiv: 1712.07151 [gr-qc].

[13] Z. Ficek and R. Tanaś. “Entangled states and collective nonclassical effects in two-atom systems.” In: *Physics Reports* 372.5 (2002), pp. 369 –443. DOI: https://doi.org/10.1016/S0370-1573(02)00368-X.

[14] H.P. Breuer and F. Petruccione. *The Theory of Open Quantum Systems*. Oxford University Press, 2002.

[15] M. Cliche and A. Kempf. “Vacuum entanglement enhancement by a weak gravitational field.” In: *Phys. Rev. D* 83 (4 2011), p. 045019. DOI: 10.1103/PhysRevD.83.045019.

[16] Eduardo Martín-Martínez and Nicolas C Menicucci. “Cosmological quantum entanglement.” In: *Classical and Quantum Gravity* 29.22 (2012), p. 224003. DOI: 10.1088/0264-9381/29/22/224003.

[17] Grant Salton, Robert B Mann, and Nicolas C Menicucci. “Acceleration-assisted entanglement harvesting and rangefinding.” In: *New Journal of Physics* 17.3 (2015), p. 035001. DOI: 10.1088/1367-2630/17/3/035001.

[18] Stephen A. Fulling. “Nonuniqueness of canonical field quantization in Riemannian space-time.” In: *Phys. Rev.* D7 (1973), pp. 2850–2862. DOI: 10.1103/PhysRevD.7.2850.

[19] Paul Davies. “Scalar production in Schwarzschild and Rindler metrics.” In: *Journal of Physics A: Mathematical and Theoretical* 8 (1975), pp. 609–616. DOI: 10.1088/0305-4470/8/4/022.

[20] W. G. Unruh. “Notes on black hole evaporation.” In: *Phys. Rev.* D14 (1976), p. 870. DOI: 10.1103/PhysRevD.14.870.

[21] N. D. Birrell and P. C. W. Davies. *Quantum Fields in Curved Space*. Cambridge Monographs on Mathematical Physics. Cambridge, UK: Cambridge Univ. Press, 1984.

[22] B. F. Svaiter and N. F. Svaiter. “Inertial and noninertial particle detectors and vacuum fluctuations.” In: *Phys. Rev.* D46 (1992). [Erratum: Phys. Rev.D47,no.10,4802(1993)], pp. 5267–5277. DOI: 10.1103/PhysRevD.46.5267,10.1103/PhysRevD.47.4802.

[23] S. W. Hawking. “Particle Creation by Black Holes.” In: *Commun. Math. Phys.* 43 (1975), pp. 199–220. DOI: 10.1007/BF02345020.

[24] G. Rizzi and M.L. Ruggiero. *Relativity in Rotating Frames: Relativistic Physics in Rotating Reference Frames*. Fundamental Theories of Physics. Amsterdam: Springer Netherlands, 2013.

[25] G. Denardo and E. Percacci. “Quantum field theory for a rotating observer.” In: *Il Nuovo Cimento B (1971-1996)* 48.1 (1978), pp. 81–89. DOI: 10.1007/BF02748650.

[26] J. R. Letaw and J. D. Pfautsch. “Quantized scalar field in rotating coordinates.” In: *Phys. Rev. D* 22 (6 1980), pp. 1345–1351. DOI: 10.1103/PhysRevD.22.1345.

[27] J. S. Bell and J. M. Leinaas. “Electrons as accelerated thermometers.” In: *Nucl. Phys.* B212 (1983), p. 131. DOI: 10.1016/0550-3213(83)90601-6.

[28] J. S. Bell and J. M. Leinaas. “The Unruh Effect and Quantum Fluctuations of Electrons in Storage Rings.” In: *Nucl. Phys.* B284 (1987), p. 488. DOI: 10.1016/0550-3213(87)90047-2.

[29] Jason Doukas, Shih-Yuin Lin, B.L. Hu, and Robert B. Mann. “Unruh Effect under Non-equilibrium conditions: Oscillatory motion of an Unruh-DeWitt detector.” In: *JHEP* 11 (2013), p. 119. DOI: 10.1007/JHEP11(2013)119. arXiv: 1307.4360 [gr-qc].

[30] P. C. W. Davies, T. Dray, and C. A. Manogue. “The Rotating quantum vacuum.” In: *Phys. Rev.* D53 (1996), pp. 4382–4387. arXiv: gr-qc/9601034 [gr-qc].

[31] P. Ehrenfest. “Gleichförmige Rotation starrer Körper und Relativitätstheorie.” In: *Physik Zeitschrift* 10 (1909), p. 918.

[32] M. Born. “Die Theorie des starren Elektrons in der Kinematik des Relativitatsprinzips.” In: *Ann. d. Phys.* 30 (1909), p. 1.

[33] M. Planck. “Gleichformige Rotation und Lorentz-Kontraktion.” In: *Physik Zeitschrift* 11 (1910), p. 294.

[34] T. Kaluza. “Zur Relativitätstheorie.” In: *Physik Zeitschrift* 11 (1910), p. 977.

[35] A. Einstein. “Zum Ehrenfestschen Paradoxon.” In: *Physik Zeitschrift* 12 (1911), p. 509.

[36] G. Sagnac. “L’éther lumineux démontré par l’effet du vent relatif d’éther dans un interféromètre en rotation uniforme.” In: *C. R. Acad. Sci. Paris* 157 (1913), p. 708.

[37] G. Sagnac. “Sur la preuve de la réalité de l’éther lumineaux par l’expérience de l’interférographe tournant.” In: *C. R. Acad. Sci. Paris* 157 (1913), p. 1410.

[38] Bryce S. DeWitt. “Quantum field theory in curved spacetime.” In: *Physics Reports* 19.6 (1975), pp. 295 –357. DOI: 10.1016/0370-1573(75)90051-4.

[39] J. Stachel. “The rigidly rotating disk as the “missing link” in the history of general relativity.” In: *Einstein and the History of General Relativity*. 1989, pp. 48–62.

[40] C. Møller. "The Theory of Relativity." In: Oxford: Clarendon Oxford, 1969, p. 223.

[41] L. D. Landau and E. M. Lifschitz. *The Classical Theory of Fields*. Course of theoretical physics. Elsevier Science, 1975.

[42] M. G. Trocheries. "Electrodynamics in a Rotating Frame of Reference." In: *Phil. Mag* 40 (1949), p. 1143.

[43] H. Takeno. "On Relativistic Theory of Rotating Disk." In: *Prog. Th. Phys.* 7 (1952), p. 367.

[44] V. A. De Lorenci and N. F. Svaiter. "A Rotating quantum vacuum." In: *Found. Phys.* 29 (1999), pp. 1233–1264. DOI: 10.1023/A:1018807714794.

[45] V. A. De Lorenci, R. D. M. De Paola, and N. F. Svaiter. "The Rotating detector and vacuum fluctuations." In: *Class. Quant. Grav.* 17 (2000). [Erratum: Class. Quant. Grav.18,205(2001)], pp. 4241–4254. DOI: 10.1088/0264-9381/17/20/306.

[46] R D M De Paola and N F Svaiter. "A rotating vacuum and a quantum version of Newton's bucket experiment." In: *Classical and Quantum Gravity* 18.9 (2001), pp. 1799–1808. DOI: 10.1088/0264-9381/18/9/313.

[47] Ø. Grøn. "Relativistic description of a rotating disk." In: *Am. J. Ph.* 43 (1975), p. 869. DOI: 10.1119/1.9969.

[48] Ø. Grøn. "Rotating Frames in Special Relativity Analyzed in Light of a Recent Article by M. Strauss." In: *Int. J. Th. Phys.* 16 (1977), p. 603. DOI: 10.1007/BF01811093.

[49] R. Adler, M. Bazin, M. Schiffer, and C.K. Weichert. *Introduction to General Relativity*. International series in pure and applied physics. McGraw-Hill, 1965. URL: https://books.google.com.br/books?id=vHUuAAAAIAAJ.

[50] R. D. Klauber. "New Perspectives on the Relativistically Rotating Disk and Non-Time-Orthogonal Reference Frames." In: *Found. Phys. Lett.* 11 (1998), p. 405. DOI: 10.1023/A:1022548914291.

[51] Charles T. Ridgely. "Applying relativistic electrodynamics to a rotating material medium." In: *American Journal of Physics* 66.2 (1998), pp. 114–121. DOI: 10.1119/1.18828. eprint: https://doi.org/10.1119/1.18828.

[52] E. E. Phipps. "Kinematics of a "rigid" rotor." In: *Lett. Nuovo Cimento* 9 (1974), pp. 467–470. DOI: 10.1007/BF02819912.

[53] A. Brillet and J. L. Hall. "Improved Laser Test of the Isotropy of Space." In: *Phys. Rev. Lett.* 42 (9 1979), pp. 549–552. DOI: 10.1103/PhysRevLett.42.549. URL: https://link.aps.org/doi/10.1103/PhysRevLett.42.549.

[54] Robert D. Klauber. "Analysis of the anomalous Brillet and Hall experimental result." In: *Found. Phys. Lett.* 17 (2004), pp. 125–147.

[55] N. F. Svaiter. "Teoria Quântica de Campos em Sistemas de Coordenadas Curvilíneas no Espaço-Tempo de Minkowski e em Espaços Curvos." CBPF - Centro Brasileiro de Pesquisas Físicas, 1989. URL: http://cbpfindex.cbpf.br/index.php?module=main&moduleFile=pubDetails&pubId=6421&typeId=9.

[56] Viatcheslav Mukhanov and Sergei Winitzki. *Introduction to quantum effects in gravity*. Cambridge University Press, 2007. ISBN: 978-0-521-86834-1, 978-1-139-78594-5.

[57] Robert M. Wald. *Quantum Field Theory in Curved Space-Time and Black Hole Thermodynamics*. Chicago Lectures in Physics. Chicago, IL: University of Chicago Press, 1995. ISBN: 978-0-226-87027-4.

[58] Leonard Parker and David Toms. *Quantum Field Theory in Curved Spacetime: Quantized Fields and Gravity*. Cambridge Monographs on Mathematical Physics. Cambridge University Press, 2009. DOI: 10.1017/CBO9780511813924.

[59] S.A. Fulling. *Aspects of Quantum Field Theory in Curved Space-time*. Vol. 17. 1989.

[60] Sean M. Carroll. *Spacetime and Geometry*. Cambridge University Press, 2019. ISBN: 978-0-8053-8732-2, 978-1-108-48839-6, 978-1-108-77555-7.

[61] Charles W. Misner, K.S. Thorne, and J.A. Wheeler. *Gravitation*. San Francisco: W. H. Freeman, 1973. ISBN: 978-0-7167-0344-0, 978-0-691-17779-3.

[62] H. Umezawa. *Advanced field theory: Micro, macro, and thermal physics*. American Institute of Physics Press, 1993.

[63] Gabriel Picanço, Nami F. Svaiter, and Carlos A.D. Zarro. "Radiative Processes of Entangled Detectors in Rotating Frames." In: (2020). arXiv: 2002.06085 [hep-th].

[64] D.W. Sciama, P. Candelas, and D. Deutsch. "Quantum Field Theory, Horizons and Thermodynamics." In: *Adv. Phys.* 30 (1981), pp. 327–366. DOI: 10.1080/00018738100101457.

[65] J. Monsair A. M. J. "Processos radiativos de estados emaranhados na presença de fronteiras." CBPF - Centro Brasileiro de Pesquisas Físicas, 2014. URL: http://cbpfindex.cbpf.br/index.php?module=main&moduleFile=pubDetails&pubId=10337&typeId=10.

[66] Eduardo Martín-Martínez, T. Rick Perche, and Bruno de S.L. Torres. "General Relativistic Quantum Optics: Finite-size particle detector models in curved spacetimes." In: *Phys. Rev. D* 101.4 (2020), p. 045017. DOI: 10.1103/PhysRevD.101.045017. arXiv: 2001.10010 [quant-ph].

[67] P G Grove and A C Ottewill. "Notes on 'particle detectors'." In: *Journal of Physics A: Mathematical and General* 16.16 (1983), pp. 3905–3920.

[68] Huabing Cai, Zhen Li, and Zhongzhou Ren. "Resonance interaction between uniformly rotating two-level entangled atoms." In: *Eur. Phys. J. Plus* 133.11 (2018), p. 458. DOI: 10.1140/epjp/i2018-12266-8.

[69] C. D. Rodríguez-Camargo, N. F. Svaiter, and G. Menezes. "Finite-time response function of uniformly accelerated entangled atoms." In: *Annals Phys.* 396 (2018), pp. 266–291. DOI: 10.1016/j.aop.2018.07.002. arXiv: 1608.03365 [quant-ph].

[70] Stanislaw Kryszewski and Justyna Czechowska-Kryszk. *Master equation - tutorial approach*. 2008. arXiv: 0801.1757 [quant-ph].

[71] L Ford, N Svaiter, and M Lyra. "Radiative properties of a two-level system in the presence of mirrors." In: *Phys. Rev.* A49 (1994), pp. 1378–1386. DOI: 10.1103/PhysRevA.49.1378.

[72] T. T. Fraenkel. *Gravitational Curvature: An introduction to Einstein's theory*. W. H. Freeman and Company, 1979.

[73] Lee Hodgkinson, Jorma Louko, and Adrian C. Ottewill. "Static detectors and circular-geodesic detectors on the Schwarzschild black hole." In: *Phys. Rev.* D89.10 (2014), p. 104002. DOI: 10.1103/PhysRevD.89.104002.

COLOPHON

This document was typeset using the typographical look-and-feel `classicthesis` developed by André Miede and Ivo Pletikosić. The style was inspired by Robert Bringhurst's seminal book on typography "*The Elements of Typographic Style*". `classicthesis` is available for both LaTeX and LyX:

https://bitbucket.org/amiede/classicthesis/

Happy users of `classicthesis` usually send a real postcard to the author, a collection of postcards received so far is featured here:

http://postcards.miede.de/

Thank you very much for your feedback and contribution.